Soft nanoparticles (thermo-responsive nanogels and bicelles) with biotechnological applications: From synthesis to simulation through colloidal characterization

ARTICLE *in* SOFT MATTER · JUNE 2011

Impact Factor: 4.03 · DOI: 10.1039/c0sm01409e

7 AUTHORS, INCLUDING:

Jose Ramos
Imperial College London & POLYMAT-Unive…
29 PUBLICATIONS **598** CITATIONS
SEE PROFILE

Lucyanna Barbosa-Barros
University of Barcelona
22 PUBLICATIONS **289** CITATIONS
SEE PROFILE

Joan Estelrich
University of Barcelona
122 PUBLICATIONS **1,823** CITATIONS
SEE PROFILE

Jacqueline Forcada
Universidad del País Vasco / Euskal Herriko…
78 PUBLICATIONS **1,648** CITATIONS
SEE PROFILE

Soft Matter

View Online
Dynamic Article Links

Cite this: *Soft Matter*, 2011, **7**, 5067

www.rsc.org/softmatter

REVIEW

Soft nanoparticles (thermo-responsive nanogels and bicelles) with biotechnological applications: from synthesis to simulation through colloidal characterization

Jose Ramos,[a] Ainara Imaz,[b] José Callejas-Fernández,[a] Lucyanna Barbosa-Barros,[c] Joan Estelrich,[c] Manuel Quesada-Pérez[d] and Jacqueline Forcada*[b]

Received 2nd December 2010, Accepted 6th February 2011
DOI: 10.1039/c0sm01409e

The use of nanotechnology in biotechnological applications has attracted tremendous attention from researchers. Currently many nanomaterials, such as soft nanoparticles, are under investigation and development for their use in biomedicine. Among soft nanoparticles, polymeric gels in the nanometre range, known as nanogel particles, have received considerable attention. Nanogel particles, which are formed by polymeric chains loosely cross-linked to form a three-dimensional network, swell by a thermodynamically good solvent but do not dissolve in it. Nanogels are composed of hydrophilic polymers capable of undergoing reversible volume-phase transitions in response to environmental stimuli. Among them, temperature-sensitive nanogels showing a volume phase transition temperature (VPTT) near physiological temperature have been investigated in detail. Nanogels based on biocompatible and temperature-sensitive polymers having a lower critical solution temperature (LCST) around 32 °C in aqueous solutions swell at low temperatures and collapse at high ones. This unique behavior makes these nanogels attractive for pharmaceutical, therapeutical, and biomedical applications. In this review, different synthesis strategies to produce this type of nanogels in dispersed media are revised. Special attention is paid to poly(*N*-vinylcaprolactam) (PVCL)-based nanogels due to their proven biocompatibility. On the other hand, an extensive review on the characteristics, preparation, and physicochemical properties of another type of soft nanoparticles, which are the bicelles, is presented. The different morphologies obtained depending on experimental conditions such as temperature, lipid concentration, and long- and short-chain phospholipids molar ratio are revised, emphasizing on an important property of bicelles: their alignment in the presence of a magnetic field, and presenting the most important applications of bicelles as membrane models in diverse conformational studies of proteins and membrane peptides, together with the possibilities of administration of such vesicles by systemic routes. A key challenge for the characterization of both soft nanoparticles (nanogels and bicelles) involves the elucidation of their colloidal properties. In this work, some colloidal features of these nanoparticles such as their size, electric double layer or the internal structure and motions of their chains are analyzed. In addition, an overview on the previous and current understanding of the methods and techniques employed in this colloidal characterization is presented, mainly from an experimental point of view. Finally, the most recent results on polyelectrolyte gels and bicelles obtained from computer simulations are also briefly commented. Concerning polyelectrolyte gels, this review is mainly focused on the most important feature of these systems, their large capacity of swelling, which has been explored by simulation in the last decade.

[a]*Grupo de Física de Fluidos y Biocoloides, Departamento de Física Aplicada, Facultad de Ciencias, Universidad de Granada, 18071 Granada, Spain*
[b]*Grupo de Ingeniería Química, Institute for Polymer Materials POLYMAT, Facultad de Ciencias Químicas, Universidad del País Vasco/EHU, Apdo. 1072, Donostia-San Sebastián, 20080, Spain. E-mail: jacqueline.forcada@ehu.es; Fax: +34-943-015-270; Tel: +34-943-018-182*
[c]*Departament de Fisicoquímica, Facultat de Farmàcia, Universitat de Barcelona, 08028 Barcelona, Spain*
[d]*Departamento de Física, Escuela Politécnica Superior de Linares, Universidad de Jaén, 23700 Linares, Jaén, Spain*

1. Introduction

Among the broad research fields in nanotechnology, nanogel particles have received considerable attention. The term nanogel describes cross-linked polymer particles of nanometric size and their distinct property is the ability to swell in a thermodynamically good solvent.[1] The broad range of applications of nanogels arises from their stimulus–responsive nature and many different

stimuli have been investigated for environmentally sensitive nanogels. Among them, temperature-sensitive nanogels are one of the most studied systems.[2] Poly(*N*-isopropylacrylamide) (PNIPAM) and poly(*N*-vinylcaprolactam) (PVCL) are temperature responsive polymers which undergo a conformational transition in aqueous media at a critical temperature, known as the lower critical solution temperature (LCST), of approximately 32 °C (Fig. 1). PNIPAM is the most widely studied temperature-sensitive polymer,[3] but in spite of the large amount of applications of PNIPAM-based nanogels reported,[4–12] the use of PNIPAM as a biomaterial may be limited because of its higher cytotoxicity and its lower cell viability with respect to PVCL,[13] thus its application in drug delivery systems may be extremely restricted.[14] The nature of the particle surface is the primary factor that affects the interactions between the cell membrane and the particle. Surface properties of neutral PVCL and PNIPAM aggregates have been studied by Laukkanen *et al.*[15] concluding that the surface of PVCL particles at elevated temperatures is actually hydrophilic. PVCL is a relatively new type of nonionic water-soluble polymer that undergoes heat-induced phase separation in water, and due to its higher hydrophilicity is well tolerated at a broad range of polymer concentrations (0.1–10.0 mg mL^{-1}) after 3 h of incubation at room temperature, at physiological temperature (37 °C). In addition, the biocompatibility of PVCL-based nanogels was also proved by Imaz and Forcada[16] concluding their suitability to be used in biotechnological applications.

Relatively new kind of self-assembling structures, which share characteristics of liposomes and micelles, are the bicelles.[17,18] These nanoparticles are formed by two kinds of phospholipids, one with a large hydrocarbon chain that forms bilayers over a wide range of temperature and water content, and the other with a short hydrocarbon chain that generally form micelles. The ratio between the molar concentration of the long-chain phospholipid over the molar concentration of the short-chain phospholipid is defined as q. Binary mixtures of both phospholipids at a suitable molar ratio q tend to form aggregates that consist of disc-shaped particles, the bicelles (or *bi*layered mi*celles*). The edges of the disks would contain the short-chain phospholipids whereas the long-chain phospholipids would form the central part of the disks (Fig. 2).

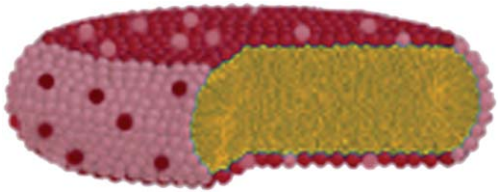

Fig. 2 Schematic representation of a bicelle. Pink: phospholipids of short-chain. Deep red: phospholipids of long-chain.

The characterization and knowledge of the colloidal properties of these nanoparticles are crucial for their applications (as individual entities or forming diverse structures). In spite of the outstanding interest of both PVCL-based nanogels and bicelles, it is quite surprising that only a few works can be found in the literature dealing with size, charge, electric double layer, aggregation phenomena, internal structure or the motions of their components. Whereas the study of PVCL-based nanogels has been promoted by the accumulated experience acquired with the well-known PNIPAM-based nanogels,[1,2,6,19] the study of bicelles from a colloidal point of view is still pending.[17,18,20] For this characterization, scattering techniques, such as Light Scattering (LS), Small Angle Neutron Scattering (SANS) and Small Angle X-Ray Scattering (SAXS), play a fundamental role as well as the image analysis obtained *via* SEM, TEM, and AFM. This review is focused mainly on LS and SANS-SAXS characterizations because LS together with image analysis is able to determine the overall dimensions of the nanoparticles and SANS-SAXS are well suited to study their internal structure.

Needless to say, computer simulations are currently a powerful tool for achieving better understanding of the behavior of soft matter.[21,22] Concerning gels, simulations of cross-linked (polymer) networks date back to the 1980s. These works were reviewed by Escobedo and de Pablo.[23] However, the simulation of polyelectrolyte gels is mainly restricted to the last decade and, in general, only an inner piece of gel (replicated periodically) is simulated to avoid an extremely large number of particles in the simulation cell. At any rate, most of the results obtained for a piece of gel can be indistinctly applied to macroscopic gels or nanogels if border effects are neglected. Regarding bicelles,

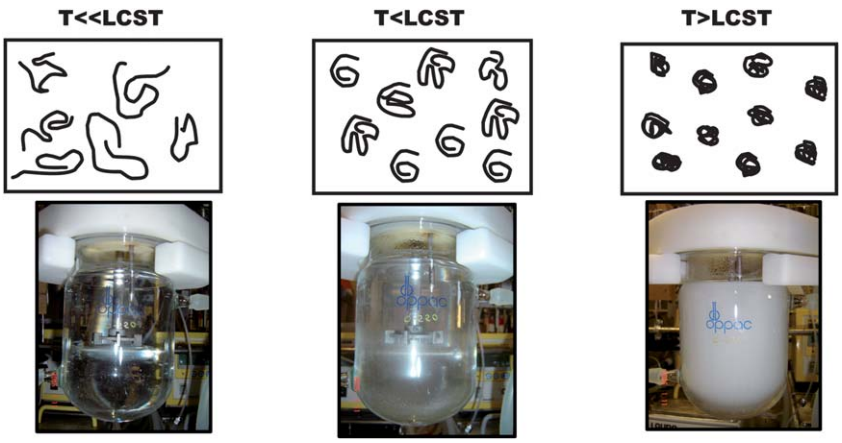

Fig. 1 Conformational transitions in aqueous media for temperature-sensitive polymers. From left to right: reaction medium temperature below, near, and above the LCST.

simulations of these systems have only appeared on stage during the last five years. The last part of this work is precisely devoted to recent simulations of polyelectrolyte gels and bicelles.

2. Synthesis procedures

2.1. Synthesis of PVCL-based thermo-responsive nanogels

PVCL-based nanogels are prepared by free radical polymerization of VCL monomer. Although many authors were motivated to prepare and characterize linear PVCL homopolymers and copolymers in solution using different solvents, few groups have synthesized the cross-linked ones in aqueous phase. Table 1 summarizes the reagents and reaction conditions used in different syntheses carried out in dispersed media to produce cross-linked VCL-based nanogels.

Regarding VCL-based nanogels, no more than 25 works have been published in the last ten years. Among them, in 1999 the group of Wu prepared PVCL-based nanogels by free radical polymerization in water and using *N*,*N*′-methylenebisacrylamide (MBA) as cross-linker, sodium dodecyl sulfate (SDS) and *N*-dodecylpyridinium bromide (DPB) as emulsifiers, and potassium persulfate (KPS) and *tert*-butyl hydroperoxide (TBHPO) as initiators.[24] The aim of this work was to study the effect of both anionic and cationic surfactants on the swelling and shrinking of the nanogels. Later, they carried out polymerizations to produce VCL- and sodium acrylate (NaA)-based nanogels in water.[25–27] The cross-linker and emulsifier used were the same as in the previous case: MBA and SDS, respectively. In 2007, Vihola *et al.*[28] prepared core–shell polymer particles consisting of temperature-responsive nanoparticles with an inner hydrophobic fluorescent polystyrene (FPS)-containing core and thermo-responsive PVCL-based nanogel shell. First, the fluorescent core particles were prepared by radical polymerization of styrene and fluorescein dimethacrylate in water. In the following step, VCL, cross-linker (MBA), initiator 2,2′-azobis [2-methyl-*N*-(2-hydroxyethyl) propionamidine] (VA-086) and the seed FPS-latex dispersion were mixed, and the polymerization reactions were allowed to proceed at 70–80 °C for 3 h. The main objective of this work was to analyze cell–polymer interactions of thermo-responsive poly(VCL) coated particles. PVCL enhanced the cellular attachment of FPS-particles as a function of temperature presumably by hydrophobic interactions with lipophilic cell membranes. Boyko *et al.*[29] obtained PVCL-based nanogels stabilized with different molecular weights of poly(vinyl alcohol) (PVA). MBA and 2,2′-azobis(2-methylpropionamidine) (AMPA) were used as cross-linking agent and initiator, respectively. They concluded that PVA stabilization of PVCL nanogel dispersions differs from attached stabilization of insoluble polymers due to the weak adsorption of the hydrophobic part of PVA on PVCL chains. They also synthesized nanogels without stabilizer but adding *N*-vinylpyrrolidone (VP) as comonomer[30] with the aim to study the influence of the temperature on the size of these nanogels by the combined static and dynamic light scattering (SLS/DLS) and small angle neutron scattering (SANS). Laukkanen *et al.*[31] prepared cross-linked nanoparticles of PVCL grafted with poly(ethylene oxide)bismethacrylate (PEObismethacrylate) in water by using MBA as cross-linker, SDS as emulsifier and KPS as initiator. Imaz and Forcada have also been active during the last few years in the synthesis of PVCL-based nanogels[32–34] reporting the synthesis of different families of nanogels such as poly(VCL-*co*-MBA), poly(VCL-*co*-MBA-*co*-3-*O*-methacryloyl-1,2:5,6-di-*O*-isopropylidene-α-D-glucofuranose (3-MDG)), and poly(VCL-*co*-poly(ethylene glycol diacrylate) (PEGDA)). In these polymerizations, apart from using SDS and KPS as emulsifier and initiator, respectively, an additional reagent was employed: a buffer, $NaHCO_3$. Imaz and Forcada[32] also studied the effect of surfactant on the average diameters of nanogel nanoparticles and on their VPTTs. All the SDS concentrations used were below the critical micelle concentration in water. They observed that 1 wt% of SDS with respect to the monomer was not enough to obtain stable nanogel particles. Moreover as expected, the higher the amount of surfactant, the smaller the final average diameter obtained (at 55 °C). Other relevant authors in this field are Pich and coworkers. In 2003, they synthesized thermo-sensitive nanogels by surfactant free emulsion copolymerization of VCL and acetoacetoxy ethyl methacrylate (AAEM) in water with AMPA azo-initiator.[35] In another attempt, these nanogels were used as template for oxidative polymerization of pyrrole.[36] It was found that pyrrole polymerization takes place directly in the nanogel network leading to formation of composite particles. The nanogels so obtained showed fully reversible collapse–swelling properties. In 2006, they synthesized temperature- and pH-sensitive nanogels by functionalizing P(VCL-*co*-AAEM) with vinylimidazole (VIm).[19] Nanogel particles swell at pH = 4 and the swelling can be controlled by the VIm content in the microgel. In a recent publication,[37] the synthesis of polyampholyte nanogels based on copolymers of VCL, itaconic acid dimethyl ester (IADME), and VIm was reported. After hydrolysis of the ester groups of

Table 1 Reagents and reaction conditions used to produce thermo-responsive cross-linked *N*-vinylcaprolactam (VCL)-based nanogels in dispersed media

Monomers	Buffer	Cross-linkers	Emulsifiers	Initiators	Reaction conditions	References
VCL	—	MBA	SDS; DPB	KPS; TBHPO	70 °C, 20 h; 108 °C, 30 h	24
VCL, NaA	—	MBA; —	—; SDS	KPS	60 °C, 24 h	25–27
VCL, FPS (seed)	—	MBA	—	VA-086	70–80 °C, 3 h	28
VCL	—	MBA	PVA	AMPA	70 °C, 8 h	29
VCL, VP	—	MBA	—	AMPA	70 °C, 8 h	30
VCL, PEObismethacrylate	—	MBA	SDS	KPS	70 °C, 22 h	31
VCL; 3-MDG	$NaHCO_3$	MBA; PEGDA	SDS	KPS	70 °C, 5 h	32–34
VCL, AAEM; VIm; pyrrole	—	MBA	—	AMPA	70 °C, 8 h	35,36,19
VCL, VIm, IADME	—	MBA	—	AMPA	70 °C, 8 h	37

IADME, they obtained amphoteric nanogels having carboxylic and basic groups in the polymer network. These nanogels exhibit high colloidal stability at different pHs.

It is well known that PVCL ring is stable and does not hydrolyze in water at high temperature.[38] However, VCL ring can suffer hydrolysis during polymerization. Imaz *et al.*[39] focused on the hydrolysis of VCL and the way of avoiding it; concluding that when VCL was polymerized by emulsion polymerization and the initiator used was KPS, it was necessary to control the pH of the reaction medium in order to prevent the hydrolysis of VCL. In the absence of buffer, at low pHs, the hydrolysis percent of this monomer increases whereas by adding a buffer to the reaction medium it was avoided.

The volume phase transition behavior (value and breadth of the de-swelling transition) of the nanogel particles can also be controlled by incorporating in the polymerization recipe functional monomers or through copolymerization with more hydrophilic or more hydrophobic comonomers.

Mikheeva *et al.*[40] conducted some measurements by using high-sensitivity-differential scanning calorimetry (HS-DSC) and observed that aqueous PVCL gels undergo two heat-induced transitions: a low-temperature transition at 31.5 °C and a higher one around 37.5 °C. The first transition attributed to a micro-segregation of hydrophobic domains, whereas the second one corresponded to the gel collapse.

Gao *et al.*[24] studied the effect of both anionic (SDS) and cationic (DPB) surfactants on the swelling behavior of anionic and neutral PVCL nanogels and compared with the results obtained with PNIPAM. They observed that the addition of SDS leads to an additional swelling of the ionic and neutral PVCL nanogels at low temperatures and shifts the collapsing temperature higher. The same effect was observed for the PNIPAM nanogel/SDS system due to the formation of micelles inside the nanogel particles. The repulsion between the negatively charged SDS micelles inside the particles provoked the additional swelling. Moreover, the shrinking temperature in the presence of DPB is lower due to the neutralization of the negatively charged anionic PVCL nanogels.

Imaz and Forcada[34] synthesized VCL- and 3-MDG-based nanogels. Different ratios of 3-MDG to VCL were used and an increase in concentration of the sugar-based monomer results in a broadening of the temperature range over which de-swelling occurs. 3-MDG is a hydrophobic monomer and by copolymerizing with VCL confers hydrophobicity to the nanogel particles, decreasing the swelling extent.

Regarding bioapplications, there is a large amount of work done using PNIPAM-based nanogels for drug delivery systems[4–10] and for the uptake and release of diverse heavy metal ions[11] and macromolecules.[12] However, as noted earlier the use of PNIPAM as a biomaterial should be restricted. On the contrary, biocompatibility of PVCL determines its use in bioapplications. It was first used in cosmetic materials,[41–43] such as hair lacquer and hairspray, and since then many other applications have been found for PVCL homopolymers and gels: coatings[44] and non-particulate substrate surfaces,[45] dispersing agents,[46] thermoreversible thickeners,[47] membranes,[48] anti-cancer drug carriers.[49] Crespy *et al.*[50] synthesized VCL-based copolymers and subsequently grafted on cotton fabrics, obtaining yield responsive fabrics. These fabrics were suggested to use to modulate the skin microclimate under textiles. Moshaverinia *et al.*[51] synthesized VCL-containing acrylic-itaconic acid terpolymer for applications in glass-ionomer dental cements.

2.2. Synthesis, characteristics and properties of bicelles

A typical preparation of bicelles involves hydrating the desired mixture of long- and short-chain phospholipids, followed by a series of cycles of freezing, thawing, and gentle vortexing until a clear solution is obtained. The archetypal model of bicelles is formed by dimyristoyl-phosphatidylcholine (DMPC) as large-chain phospholipid, and dihexanoyl-phosphatidylcholine (DHPC) as short-chain one. However, to imitate better the environment of biological membranes, bicelles with different lipid compositions have been prepared. In this way, DMPC can be doped with phospholipids that have identical chain lengths but different headgroups (*e.g.*, dimyristoyl-phosphatidylglycerol (DMPG), dimyristoyl-phosphatidylserine (DMPS), dimyristoyl-phosphatidylethanolamine (DMPE),[52–54] DMPC[55] or with cellular lipids such as cholesterol and cardiolipin).[56] Bicelles can also be prepared with dipalmitoyl-phosphatidylcholine (DPPC) or dilauryl-phosphatidylcholine (DLPC) to vary the total bilayer thickness, or with an unsaturated lipid, palmitoyl-oleoyl-phosphatidylcholine (POPC) to obtain bicelles capable of forming micrometre-scale lipid domains.[57] Apart from DHPC, the rim of bicelles can be formed by a bile-salt derivative such as 3-(cholamidopropyl)dimethylammonio-2-hydroxy-1-propanesulfonate (CHAPSO).[58] The so-called ideal bicelle model supposes a strict segregation between the two main phospholipids.[59]

The size and orientation and morphological properties of these lipid aggregates vary as a function of q, the total lipid concentration (c_L), and the temperature[60,61] providing a variety of bicelle phases. Table 2 summarises the relationship among q ratio, lipid concentration, size, aggregation states and response to a magnetic field.

The alignment of bicelles is driven by the interaction between the magnetic field and the magnetic susceptibility anisotropy of the bicellar self-assembly, aided by cooperative interactions between adjacent lamellae.[74] For DMPC/DHPC bicelles, because of their net negative magnetic susceptibility anisotropy, the spontaneous direction of alignment is such that the normal to the planar lipid bilayer region lies perpendicular to the direction of the magnetic field (B). This is referred to as negative magnetic alignment. However, in the presence of surface-bound lanthanides having a positive magnetic susceptibility, such as Tm^{3+}, Yb^{3+}, Er^{3+}, and Eu^{3+}, the direction of alignment is such that the normal to the planar bilayer region lies parallel to the direction of the magnetic field. This is referred to as positive magnetic alignment and is particularly useful for solid-state Nuclear Magnetic Resonance (NMR) studies of membrane proteins to examine both the orientation of a peptide associated with the bicelle with respect to the bicelle surface and the effects of the peptide on lipid packing within the bicelle.[72,74–80] In these cases the orientation of the samples can be better assessed by ^{2}H NMR as the ^{31}P NMR can be confusing with the presence of paramagnetic shift agents that usually are placed in the vicinity of the phosphorus atoms.[81] One of the limitations for these studies is that lanthanides might bind to negatively charged sites in membrane macromolecules of interest, resulting in a change of

Table 2 Size, orientation and morphological properties of bicelles as a function of q ratio and lipid concentration at temperatures above the transition temperature of the long-chain phospholipid (DMPC)

q ratio	Lipid concentration (c_L)	Diameter/nm	Shape	Behavior in magnetic field	References
0.5–1	15%	8–10 nm	Spherical	Non-alignment	59,62–69
2	3%	~7.6 nm	Disk like	Non-alignment	16
2	10–25%	>500 nm	Ribbon like	Non-alignment	70,71
>2.3	3–40%	Variable	Disk like, ribbon like, lamellar sheets	Alignment	72,73
3.0	<3%	>500 nm	Ribbon like	Alignment	16
3.2	25%	~430 nm	Ribbon like and perforated lamellar sheets	Alignment	70
3.5	10–20%	>500 nm	Lamellar sheets	Alignment	71

conformation. This can be overcome by the incorporation into the bicellar system of a phospholipid molecule that strongly binds or chelates the lanthanides, such as phospholipids complexed with Yb^{3+}.[54] Studies with gramicidin A demonstrated that chelate sequesters the lanthanide away from the peptide binding sites. The use of DMPE-DTPA chelated in positive aligned Yb^{3+}-doped bilayers has been also tested for two membrane-associated peptides with resulting well aligned and stable spectra.[82]

The non-alignable bicelles are much smaller than their alignable counterparts and remain discoidal with segregated lipid pools.[59,68,69] These bicelles, also so-called isotropic or fast-tumbling bicelles, exist over a wide range of sample conditions and have a viscosity amenable to solution-state studies of structure of peptides and proteins.[83]

Thus, bicelles offer a unique system in which different techniques can be employed to examine the interaction of protein and model membranes. The aligned phase bicelles, $q \geq 2.3$, allow the use of solid state NMR techniques, whereas isotropic bicelles can be used to conduct high-resolution NMR studies of protein structure.[83]

In both cases, the protein sees the identical structure and environment. Therefore, the results should be directly comparable. That is, bicelles are a model that allows one to study both function and structure in the same system. Other model membranes, such as liposomes or micelles, are not suitable for high-resolution NMR studies of membrane-associated peptides and proteins since the overall vesicular reorientation rates are too low and this leads to significant line broadening.[57] Micelles have been used successfully in obtaining NMR data for membrane-associated peptides.[84–87] However, micelles are far from ideal in this role: the amphiphile packing in micelles is dramatically different from that of vesicles or bilayers, and, moreover, the curvature of micelle surface is also much greater than that for a liposome or membrane and may cause strain in proteins. It was shown that the position of a peptide in micelles can be significantly different from its position in a phospholipid bilayer.[88,89] Since bicelle interior consists of a true lipid bilayer, this system represents a more natural environment for membrane proteins.

Bicelles were developed to solve these experimental problems of current membrane models in NMR studies of protein characterization. They allow one to study both function and structure in the same system. One of the main advantages of the bicelles is their possible use in solid and solution NMR experiments to obtain information regarding conformation, interactions and location. This is possible due to the versatility of these systems, which allow us to prepare samples with different long–short phospholipid chain ratios, giving rise to oriented or fast-tumbling bicelles. The aligned phase bicelles allow the use of solid-state NMR techniques to determine the orientation of proteins and phospholipids. The isotropic bicelles can be used to conduct NMR structural studies of the peptides and proteins.

Bicelles aligned with its normal perpendicular to the magnetic field give rise to a spectrum showing two well-resolved resonances, in which the high field one corresponds to the long chain phospholipid localized in the planar surface of the aggregate, whereas the low field resonance is attributed to the short chain phospholipid distributed in the torus.[90–92] Bicelles doped with cardiolipin or other phospholipids such as DMPE, DMPS or DMPG shows a third resonance positioned near long-chain phospholipid resonance location.

The ^{31}P NMR spectra of pure bicelles are used in the first place to diagnose the quality of the sample orientation before and after the addition of the macromolecules to be studied.[75,92–97] Titration with appropriated amount of peptide also brings valuable information on the bicelle organization. Normally membrane disruption is detected by the appearance of an isotropic resonance as observed with antibiotics[94] and melittin[98] that exert a lytic effect on bicelles. In addition, the perturbations in the phospholipid headgroup can be detected by observing the ^{31}P chemical shift anisotropy, as did Marcotte *et al.* when binding metenkephalin to zwitterionic and anionic bicelles and correlated to changes in the lipid headgroup motions.[54]

With the ^{2}H NMR it is possible to determine variations in the lipid chain order by monitoring changes in the quadrupolar splitting values, which consider several contributions such as the bicelles wobbling, intramolecular motions such as the *trans–gauche* isomerizations, and anisotropic reorientation of the phospholipid molecules.[94,99,100] It is also possible to use phospholipids with deuterated cholines to determine the effects of macromolecules in the surface of bicelles. In these cases, two doublets attributed to the α- and β-methylene close to the phosphate and trimethylamine groups compose the spectrum. The combined use of choline and chain-deuterated long chain phospholipid is useful to investigate the interaction of macromolecules with bicelles as information is obtained at the polar and apolar regions.[56,94]

Some studies carried out by Andersson and Mäler using several peptides in fast-tumbling bicelles have demonstrated that the peptide is less structured and more flexible in zwitterionic

bicelles than in anionic bicelles.[101,102] Another interesting finding is that by measuring the translational diffusion constant, in pulsed field gradient NMR, it is possible to calculate the amount of bound peptide in the sample.[103] The position of peptide in fast-tumbling bicelles can also be determined using different methods such as the inclusion of paramagnetic probes inserted in different positions in bicelles, the study of amide exchange, and the observation of NOE effects of peptide bounded to phospholipids.[62]

On the other hand, bicelles are also a promising tool for biomedical applications. In this way, their lipid composition, small size and structural versatility drew attention of some researchers to the potential use of these systems to study the stratum corneum (SC), as well as for using them as drug delivery systems.[104] As said previously, the characteristics of bicelles are different from those of liposomes and micelles. Although liposomes and micelles have been used for skin treatment,[105,106] their application is debated due to some aspects. Liposomes seem to be too large to penetrate into the narrow intercellular spaces of the SC[107] and the use of micelles involves a problem owing to the irritating effect of surfactants on the skin.[108] In this context, the use of bicelles for skin applications is clearly advantageous: their size is small enough for passing through the SC lipid lamellae, and their composition consists exclusively of lipids.[109]

In the first publication suggesting bicelles as a potential system to use in skin,[109] ceramides were included in bicelles of DMPC/DHPC, $q = 2$, $c_L = 20\%$. Ceramides organized in domains along bicelles, which allowed the inclusion of up to 10% w/w of ceramide without affecting its structural integrity. The morphological effects of ceramides in DMPC/DHPC bicelles were observed using electron microscopy techniques and dynamic light scattering. The results indicated that the inclusion of ceramide induced the formation of twisted zones in small bicelles. At higher concentrations, ceramides would promote the branching of the aggregates.[110] Since ceramides are the dominant lipid component of epidermal stratum corneum, bicelles including ceramides would be useful as a model membrane for the study of stratum corneum lipids behavior.

More recently, it was reported the effect of the interaction of bicelles of DMPC/DHPC, with a molar ratio $q = 2$ with the skin.[104] Bicelles had dimensions of 16 nm in diameter and 4.5 nm in thickness, compatible with an isotropic discoidal system. In that work, fresh human skin was incubated with bicelles and then studied by Freeze Substitution Transmission Electron Microscopy (FSTEM). In parallel, biophysical properties of skin, such as transepidermal water loss (TEWL), elasticity, skin capacitance and irritation were measured in healthy skin *in vivo*. Considering the structure of SC, the pass of small bicelles through the lipid region seems reasonable.[111] The *in vivo* assay showed that bicelles increased the permeability and elastic parameters without promoting irritation of the skin *in vivo*. The application of bicelles promoted the increase in skin permeability and consequently the increase in the TEWL values, probably because of differences in the transition temperature of skin lipids (about 37 °C)[112] and phospholipids from bicelles (about 23 °C).[113] The incorporation of the phospholipids from bicelles into SC lipid lamellae could induce the transition of the lipid lamellar structures of the skin from gel state to liquid crystalline. At this regard, bicelles could have similar effect as some penetration enhancers, which cause phase transformations in the lipid domains that may be relevant in the context of skin permeation.[114]

In another study, bicelles of DPPC/DHPC $q = 3.5$, $c_L = 20\%$ were incubated with fresh pigskin. Bicelles had about 15 nm in diameter and 5.4 nm of thickness. Cryo-SEM showed structural changes in the lipid lamellae regions with the presence of vesicle structures of about 200 nm and lamellar like structures with irregular shapes, indicating that these bicelles were able to penetrate the skin SC *in vitro* and to grow, forming vesicles inside the intercellular lipid spaces. These results are apparently inconsistent with the ones observed with bicelles composed by DMPC/DHPC $q = 2$ mentioned above.[104] The *in vitro* analysis of the SC incubated with these bicelles did not show vesicle formation or lamellar structures, neither microstructural modifications. This fact can be explained by the lower T_m of DMPC (23 °C) in comparison with the temperature of incubation of SC with bicelles (37 °C). At this temperature, the bicelles were in the fluid phase, therefore forming large aggregates that could not penetrate through the narrow intercellular spaces of the SC, and their effects were concentrated in the skin surface. Indeed, no microstructural changes in the SC were visualized in that investigation. By contrast, the bicelles made up of DPPC/DHPC (T_m of DPPC of 41 °C) were in gel phase, therefore forming small aggregates at the temperature of incubation. These aggregates were able to penetrate in the skin SC. The presence of vesicles in the intercellular spaces of the SC was attributed to a structural transition process from bicelles to vesicles occurring inside the tissue. Once inside the SC, bicelles would have grown forming vesicles and lamellar-like structures due to a dilution process.[110]

To observe more deeply the effect of the bicelles on the skin, a study was conducted using techniques such as attenuated total reflectance-Fourier transform infrared (ATR-FTIR) spectroscopy and grazing incidence small and wide X-ray scattering (GISAXS and GIWAXS).[115] It was found that the treatment of the skin with bicelles caused a phase transition of the SC lipids from the gel state to the liquid-crystalline state. This transition would be promoted by the penetration of bicelles in the SC and the incorporation of its phospholipids in the SC lipid lamellar structure. This finding would explain the increase of skin permeation observed by Barbosa-Barros *et al.*[104] with bicelles formed by DMPC/DHPC $q = 2$. The transition from gel state to the liquid-crystalline state involves an increase in the fluidity and/or disorder of the lipids that would explain the increase of skin permeation.

Bicelles accurately fulfill the requirements for an effective skin carrier due to their size, structure, and composition. Moreover, due to the bicelles' capacity to increase the permeability parameters of the SC,[104] they could also act as an enhancer for the penetration of hydrophilic components dissolved in the aqueous medium. Further, the conversion of bicelles into vesicles inside the SC hinders their migration outside the tissue and allows for a lipid reinforcement effect in the skin and for the retention of substances inside the SC intercellular spaces, which could be very useful to intensify the effect of specific compounds carried by bicelles in the SC layers. *In vivo*, the driving force for the rearrangement of the bicellar lipids would be the hydration gradient across the skin, which varies from 15 to 29% in the SC and reaches 70% in the stratum granulosum.

Rubio *et al.*[116] reported the percutaneous absorption of the non-steroidal anti-inflammatory diclofenac diethylamine. The drug seemed to promote some rigidity in bicelle's structure, and this fact resulted in a lower penetration of the drug in comparison with the drug applied in aqueous solution. However, if the skin was pretreated with bicelles and then the aqueous solution of the drug was applied, a notorious increase in the penetration was observed. Hence, bicelles have a potential enhancement or retardant effect on percutaneous absorption, which is an interesting strategy in drug delivery.

The application of these systems as carriers for administration through the systemic route or in situations where the water content of the medium is high may suppose a challenge. It is extensively reported that under dilution small bicelles become large structures. In order to overcome this difficulty, a new strategy has been recently proposed.[117] This strategy consists of the encapsulation of bicelles in lipid vesicles forming structures termed *bicosomes*. This encapsulation produced the isolation and protection of bicelles entrapped into vesicles from dilution, preserving its size and morphology in a high water content environment. The study also showed that the injection of bicelles in the cerebrospinal fluid (CSF) of rats caused their death probably by the rapid morphological changes of these structures. However, the injection of bicosomes did not cause death, which shows that the bicosomes avoided the morphological changes of bicelles.

3. Colloidal characterization

3.1. Colloidal characterization of thermo-responsive nanogels

The overall properties of a colloidal particle such as size, molecular weight, and radius of gyration are determined performing simultaneously static (SLS) and dynamic (DLS) light scattering using commercial devices. In a typical DLS experiment,[118,119] the hydrodynamic radius R_h of a particle in a solvent is obtained *via* the measure of its translational diffusion coefficient D and applying the Stokes–Einstein equation: $R_h = kT/6\pi\eta D$ where k, T, and η are the Boltzmann constant, the temperature, the solvent viscosity, respectively. The above equation is derived assuming that the particle is isolated and suffers a pure Brownian motion. Direct and hydrodynamic interactions between particles are also neglected. Briefly, D is determined from the measure of $g_1(q,\tau)$, the normalized electric field autocorrelation function, being $q = (4\pi n/\lambda_o)\sin(\theta/2)$ the scattering vector, τ the sample time and n, λ_o, and θ the solvent refractive index, the wavelength of light in vacuum and the scattering angle, respectively. For a sample of "ideal" monodisperse particles, $g_1(q,\tau)$ is an exponential function $g_1(q,\tau) = e^{-\Gamma\tau}$ whose exponential decay is $\Gamma = Dq^2$. Thus, D is obtained from the slope of $g_1(q,\tau)$ against τ. Real systems are polydisperse and $g_1(q,\tau) = \int G(\Gamma')e^{-\Gamma'\tau}d\Gamma'$ where $G(\Gamma')$ is the weight function corresponding to a particular decay (size) Γ'. Several procedures have been proposed to invert this relation.[120]

About ten years ago, Lau and Wu published the first colloidal analysis of a PVCL-based microgel.[121] Using DLS, they reported the nowadays-typical change in the particle R_h against temperature.

On the other hand, with SLS, it is possible to obtain both the weight average molecular mass M_w and the average radius of gyration R_g of these particles.[121–123] In this case, the angular dependence of the excess absolute time-averaged scattered intensity, known as the excess Rayleigh ratio R_θ, is measured. Using dilute dispersions (with an extremely low particle concentration c, $c \to 0$) and measuring at small angles θ ($\theta \to 0$), the Zimm equation provides the values of M_w, R_g and the second virial coefficient A_2

$$\frac{Kc}{R_\theta} = \left(\frac{1}{M_w} + 2A_2c\right)\left[1 + \frac{q^2R_g^2}{3}\right] \quad (1)$$

where $K = 4\pi^2n^2(dn/dc)^2/N_A\lambda_o^4$, N_A is Avogadro's number and dn/dc the specific refractive index increment.

The knowledge of the nanogel charge and the corresponding electric double layer (e.d.l.) is an important aspect in their colloidal characterization.[124–130] The charge can derive from the initiator, the cross-linker, the used surfactants and the ionic groups spread both out and inside the particle. Hoare and Pelton[124–126] analyzed the functional group distribution of carboxylic acid groups within PNIPAM-based microgels: theoretically, *via* a kinetic model[124] and experimentally using conductimetric–potentiometric titrations, DLS and electrophoresis.[125,126] Also, Ikkai *et al.* tried to deep into this subject but using SANS measurements.[127] Schachschal *et al.*[37] reported a work devoted to PVCL nanogels using several experimental techniques and stressing the importance of NMR. Additionally, the e.d.l. of PNIPAM microgels was studied in the past[126,128–130] reporting measurements of electrophoretic mobility and theoretical analyses using either the classical or Oshima's approaches.

From SLS-DLS measurements, the study of aggregation phenomena using dispersions of PVCL nanogels was reported.[26,27,131,132] Particles made of PVCL chains with a few percent of sodium acrylate were aggregated by the addition of several cations (Na^+, Ca^{2+}, Cu^{2+} and Hg^{2+}). These studies revealed a clear shrinking of the nanogels as the cation concentration is increased and a strong temperature dependence of the average hydrodynamic radius R_h and M_w of the aggregates. But a sound study of nanogels aggregation has to deal with the spatial structure of the aggregates (measuring the aggregates fractal dimensions) and the aggregation kinetics (cluster distribution, kernel, diffusion- and reaction-limited aggregation (DLCA-RLCA) regimes) and this was partially done by some authors.[133,134] The fractal dimension of PVCL aggregates at different temperatures was found for the first time together with a study of the kinetics of reversible aggregation processes. Laukkanen *et al.*[135] studied spectrophotometrically the aggregation by barium chloride of four samples of stabilized PVCL microgels. Three of them were negatively charged as capillary electrophoresis demonstrated. They concluded that the neutral sample (sterically stabilized by poly(ethylene) oxide chains) is more stable than the charged ones. Moreover, the results for swollen and collapsed states of the microgels are different.

Regarding the internal structure of nanogels, the presence of inhomogeneities in this kind of nanoparticles was suggested by Kunz and Burchard.[136] The particle form factor $P(q)$ was measured using SLS and DLS. Their experimental data were fitted with a model consisting of a hard core and a seam of dangling chains. In 1994, Wu *et al.* studied the kinetics of formation of PNIPAM microgels and reported differences in

cross-linking density throughout the particle.[137] Kratz *et al.* enhanced this fact using SANS measurements on NIPAM microgels, showing that the correlation length decreases with increasing the cross-linking density.[138,139] They also addressed the question whether the length of the cross-linker has a significant influence on the swelling behavior and internal structure of the microgel. Varga *et al.*[140] went into the effect of cross-linking density on the structure of PNIPAM microgel *via* SLS-DLS, concluding that the internal structure of the particles depends strongly on the degree of cross-linking. At high cross-linking density the particles can be described with a Gaussian segment density distribution. If the cross-linking density decreases, a highly branched coil structure is obtained. Fernández-Barbero *et al.*[141] also analyzed PNIPAM microgels using SANS. From their experiments, they proved the existence of two clear zones in the particles corresponding to a core region of high cross-linking density and an outer shell, mainly formed by PNIPAM chains. Interestingly, the microgel swelling is determined by the shell expansion that also tends to compress the particle core. More elaborated models appeared almost simultaneously in 2004 by Saunders[142] and Stieger *et al.*[143] The first one assumes (for swollen states) a higher segment density in the inner core, which is presumably more highly cross-linked. A uniform segment distribution within the core and the shell was also assumed in this work. In the second one, a different scheme based on the approach of Pedersen–Svaneborg[144] is used: The cross-linking density decreases with increasing distance to the particle center.[143] At certain distance R, the profile has decreased to half the core density (Fig. 3).

In any case, an interesting and unsolved question arises naturally from these works: why is the core usually more dense than the outer zone? The most accepted explanation is that the rapid consumption of the cross-linker at the beginning of the reaction yields a denser core.[137] The analysis of scattering data supports this hypothesis.[137–143] But the electric nature of the polymeric chains forming certain nanogels provides an alternative explanation. The charged groups can be placed both in inner and outer regions of the particles. Depending on their localization, different local charge distributions of co- and counterions and osmotic pressures could be found within the nanogel. For instance, recent theories and simulations suggest that the charge of the core would be more compensated than the charge of the shell.[145] Based on electrostatic arguments, we might therefore think the outer region would be more expanded than the core. Olvera de la Cruz has also analyzed the relevance of electrostatic interactions in self-organization.[145] Electrostatic interactions would also justify (to a great extent) the rich phase behavior predicted for interacting microgel particles.[146]

Boyko *et al.*[29] analyzed microgels based on VCL and VP by SLS, DLS and SANS. From the dependence of the ratio between the radius of gyration R_g and hydrodynamic radius R_h against temperature, these authors assumed PVCL microgels consisting of a dense core surrounded by a diffuse corona. They suggested that dangling chains, which increase the hydrodynamic radius but have little influence on the radius of gyration, cover the surface of the microgel. The SANS intensity in the swollen state (below the LCST temperature) is fitted using two terms. The first uses the form factor for a homogeneous sphere adding a term that considers the inhomogeneity of the surface, including also

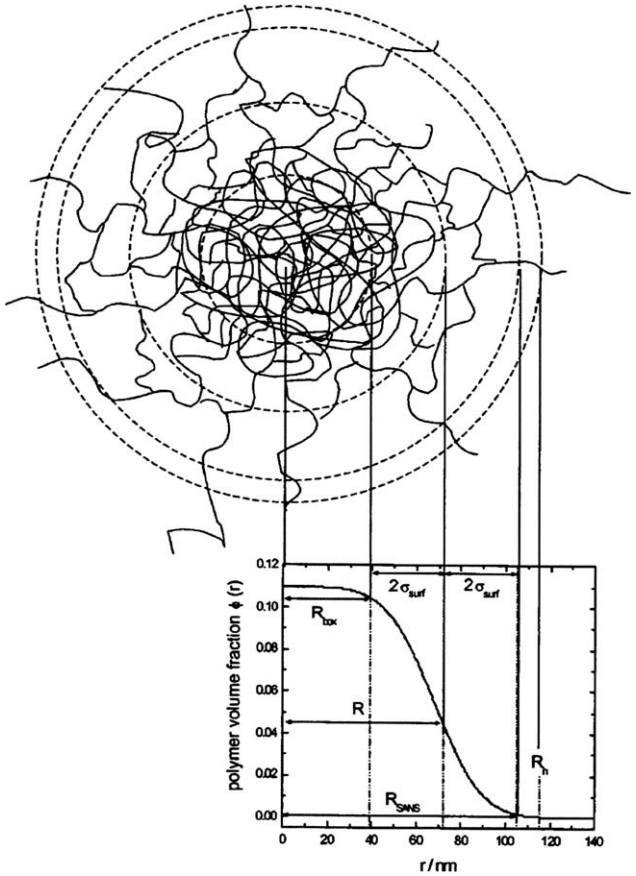

Fig. 3 Internal structure of a microgel particle. Data from ref. 143 with permission from American Institute of Physics.

the polydispersity (Gaussian particle distribution). The second term is due to the core (a Ornstein–Zernike expression is used). At the shrunk state (50 °C), Porod scattering is observed as the corona collapse onto the surface of the core.

The internal motions of chains within the microgel particle are another challenge of special interest. The mobility of flexible polymer chains in dilute solutions was theoretically and experimentally investigated using different techniques.[118,119,147–150] DLS emerged early as a suitable tool in this research.[119,147,148] As these theories predicted, the dynamic structure factor $g_1(q,\tau)$ contains contributions from the translational diffusion coefficient and the long-range internal modes of the chain motion. The relative contribution depends on the product of q and R_g of the polymer. When $qR_g \ll 1$, the translational diffusion is the dominant contribution, and the time correlation function is predicted to decay as a single exponential. As qR_g becomes larger, the various internal modes begin to contribute significantly to the correlation function $g_1(q,\tau)$, giving rise to a multiexponential time correlation function.

$$g_1(q,\tau) = \exp\left(-Dq^2\tau\right)\sum_{n=0}^{\infty} B_n(q)\mathrm{e}^{-\Gamma_n\tau} \qquad (2)$$

where D is the translational diffusion coefficient, Γ_n is the n^{th} relaxation mode and $B_n(q)$ are the weight factors for the n^{th} mode. Please note that this relation is the discrete way to write $g_1(q,\tau) = \int G(\Gamma)\mathrm{e}^{-\Gamma\tau}d\Gamma$. In the running procedure[149,150] the

inversion of $g_1(q,\tau)$ has to be done in order to find $G(\Gamma)$, using the Laplace inversion if Γ is a continuous variable or, in practice, the CONTIN inversion method. As a result, plots of $G(\Gamma)$ or normalized intensity as a function of Γ containing the different peaks (relaxation modes) are obtained.[149] These methods can also be found in the only work done on internal chain mobility of PVCL-based nanogels by Boyko *et al.*[150] At the swollen state, 15 °C, they obtained only one peak at a scattering angle of 30°, which is assigned to the translational diffusion. But at 106°, two faster relaxation peaks were found together with the diffusion peak.

3.2. Colloidal characterization of bicelles

The term "colloidal characterization" is practically unknown in the scientific literature about bicelles. This is due to the fact that these nanoparticles have emerged as an important model membrane system with broad application both in Biology and Biophysics and researchers have focused mainly on the properties of this phospholipids bilayer. Additionally, the most accepted disk morphology has a size lying in the lowest limit of colloidal domain (~30 to 50 × 4 to 5 nm). Therefore, research groups involved in colloidal science have excluded bicelles from their interest.

In this sense, it is difficult to find measurements of properties such as R_h, R_g or M_w in articles dealing with bicelles. Only one of the properties, R_h, is determined for bicelles, but just in a few works and always in routine way.[151,152] What is more, the bicelle charge, the corresponding e.d.l. and related stability-aggregation phenomena have not been studied yet from a colloidal viewpoint. Nevertheless, capillary electrophoresis measurements have been performed for suspensions of liposomes[153–155] and, more scarcely, bicelles.[156–158] But the aim of these works was mainly the separation of bicelles by size and amount of charge in order to optimize methods for membrane partitioning.[154] Their electrophoretic mobility was analyzed using old colloidal models and without including further developments. In general, ζ-potential is hardly used in these reports.[153–158] On the contrary, colloidal properties such as shape and size, and the internal structure of bicelles have been investigated directly linked to the most studied behavior of bicelles, the orientation in the presence of magnetic fields due to its diamagnetic character. Thus, NMR techniques have been widely used for the characterization of bicelles.[17,62,72,92]

Regarding the internal structure,[159–162] the study of mixtures composed mainly by a long lipid chain (DMPC or DPPC) and a short lipid chain (DHPC) started at the early 1980s. For a determined molar ratio q, both non-spherical vesicles and bilayer disks would be formed.

In 1990s, Sanders *et al.*[58,163,164] studied mixtures of long chain DMPC and short chain DHPC characterized by multinuclear (^{13}C, ^{31}P, ^{2}H) solid-state NMR. NMR spectra were shown to be consistent with the morphology of "discoidal" micelle in which DMPC is in the central part and DHPC is in the rim of the disk, respectively. Hare *et al.* analyzed bicelles made of DLPC and CHAPSO using X-ray scattering and NMR and concluded that the bilayer thickness is 3 nm, which is the same as the bilayer thickness of pure DLPC vesicles.[165] This suggests that CHAPSO does not perturb the lipid bilayer. Additionally, the orientational energy of the sample (from NMR analysis) suggests approximately 2×10^7 molecules of phospholipids per bicelle. Chung and Prestegard[166] modeled the diffusion of water as a stochastic movement over fixed sites in a lattice for a DMPC + CHAPSO system, and the results were consistent with a disk-shaped particles ~5 nm thick and having a diameter of ~20 nm. Nevertheless, as several authors point out,[58,164] NMR data do not prove unambiguously that the discoidal model is correct, but it is consistent.

In the early 2000s, the notion of "disk" has been grounded for certain phospholipids mixtures *via* SANS measurements, as can be seen in the reports of Katsaras's group.[92,151,152,167] As an example,[92] mixtures of DMPC, DHPC with and without lanthanide ions were investigated. The results revealed a wealth of distinct morphologies that were modeled using a bicellar discoidal model, an infinite stacked lamellar model and a unilamellar model, respectively. Despite the fact that the discoidal model has been widely applied for mixtures, other morphologies have been proposed. What is more, studies with NMR, SAXS and SANS confirm that the bicelle morphology depends on the q-ratio, the total weight percent of lipids, and temperature.[168,169]

The higher the value of q, the bigger is the self-assembling structure. Typical bicelles have values of q ranging from 2.5 to 5, and its lipid concentration is within 3–40 wt%. As the q-ratio or the temperature is increased (above the transition temperature (T_m) of the long-chain phospholipid), the system goes through a general sequence of structural transitions. The initially discoidal structures, found at low q and/or low temperature, transform into long somewhat flattened cylindrical micelles, which branch into networks forming wormlike micelles or ribbons, and finally condense into multilamellar sheets oriented by the magnetic field containing holes formed by short-chain phospholipids.[18,92,167,170,171] Nieh *et al.*[70] observed that samples with a total lipid content of 25 wt%, corresponding to ratios q of 5, 3.2, and 2, exhibited an isotropic (disk bicelles), a chiral nematic (long, flexible wormlike micelles or ribbons) and a lamellar phase (multilamellar vesicles) sequence on increasing temperature.

The isotropic bicelles are stable over a wide range of q ratios (q = 0.05–0.5) and temperatures (15 and 37 °C) and maintain a free (not bicelle-associated) short-chain phospholipid concentration of 7 mmol L^{-1} for DHPC. If the total phospholipid concentration is between 1 wt% and 5 wt%, the short-chain phospholipid dissociates from the bicelle to maintain the free short-chain concentration at 7 mmol L^{-1}. This increases q, which in turn, leads to a doubling of the bicelle size over this concentration range. At total phospholipid concentrations less than 1 wt%, the bicelles undergo a drastic change in morphology and all of the short-chain phospholipids leave the bicelle, causing the long-chain phospholipids to form a large soluble lipid aggregate, presumably vesicular in structure.[69]

The ideal bicelle model was challenged on the basis of detailed ^{31}P NMR studies of bicellar mixtures as a function of temperature and q by Triba *et al.*[17] that made an exhaustive study on the structural transformations of DMPC/DHPC. They showed that above a critical temperature, T_v, perforated vesicles progressively replace alignable structures. The holes in these vesicles disappear above a new temperature threshold, T_h. The driving force for these temperature-dependent transformations is the increase of DHPC miscibility in the bilayer domain above T_m. These

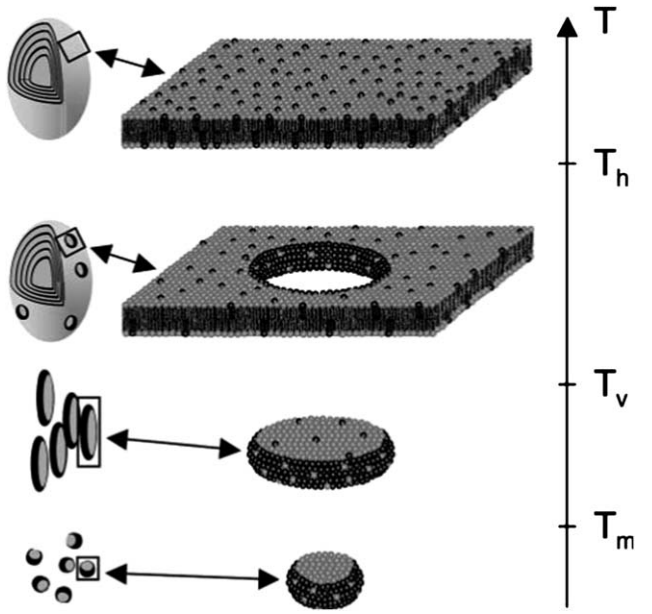

Fig. 4 Cartoon of the various DMPC/DHPC structures along with the main transition temperatures. From low to high temperatures: small segregated bicelles; larger interacting mixed bicelles; large perforated multilamellar vesicles; and large mixed multilamellar vesicles. Light lipids represent DMPC whereas dark lipids represent DHPC. The structures are represented at different scales. Data from ref. 17 with permission from Elsevier.

researchers proposed a new model called the mixed bicelle in which DHPC is finitely miscible with DMPC. A consequence of this miscibility is the rapid increase of the proportion of bilayer area when temperature is raised. Fig. 4 summarizes the transformations observed.

van Dam *et al.*[18] showed by cryo-transmission electron microscopy (cryo-TEM) that the magnetically aligning phase consisted of extended sheets with a lacelike structure. The aggregates are best described as intermediates between two-dimensional networks of flattened, highly branched, cylindrical micelles and lamellar sheets perforated by large irregular holes. The bulk of the perforated bilayer is composed of DMPC, while DHPC preferentially covers the edges of the holes. However, 20–43% of the DPHC is situated in the flat bilayer part of the aggregate, this percentage corresponds to 6–12% of the bilayer, and this number increases approximately linearly with increasing temperature, since the magnetic susceptibility anisotropy of the aggregates builds up as the bilayer grows. At temperatures above 45 °C, the aligning phase collapses.

Recently, the mixed bicelle model has been confirmed[172] by ^{1}H NMR diffusion measurements using the stimulated echo pulsed field gradient (PFG) procedure[173] of water diffusion between and across the bicellar lamellae. Results have confirmed that DPHC undergoes fast exchange between curved and planar regions as mixed bicelle model predicts.

4. Simulations of polyelectrolyte gels and bicelles

4.1. Polyelectrolyte gels (and nanogels)

Although this section is focused on the swelling behavior of polyelectrolyte gels, it should be mentioned that uncharged networks have been also studied through computer simulations and the corresponding literature includes formation of polymeric gels, dynamics of cross-linking, structural and dynamic properties and swelling. This literature was reviewed by Escobedo and de Pablo.[23] These authors also carried out simulations of uncharged hard-core networks.[174–177] It should be stressed that Escobedo and de Pablo included solvent molecules explicitly in their simulations (also modeled by hard spheres), which allowed them to study solvent mixtures and solvents at subcritical and supercritical conditions.[175,177]

To date, simulations of charged cross-linked gels are however scarce due to a combination of several factors. On the one hand, polyelectrolyte gels exhibit a considerably larger capacity of swelling. For charged gels, the swelling ratio is typically 10^2 to 10^3, whereas for uncharged gels it is approximately 10^1. These largely swollen states would require a prohibitive number of solvent particles in the simulation box. In this sense, one should also bear in mind that solvent molecules (such as water) are usually much smaller than monomeric units, which would obviously contribute to a vast number of particles in realistic simulations. For these reasons, the solvent is not explicitly considered in these simulations and the primitive model is mostly preferred. On the other hand, the long-range nature of the electrostatic interactions causes additional difficulties in the simulation of charged gels.

The first simulation of a polyelectrolyte gel dates back to 1996. Inspired by Tanaka's results,[178] Aalberts performed such simulation by using a two-dimensional finite lattice model. It should be pointed out, however, that the gel and its counterions are not described on an equal level of complexity.[179] In other words, the framework is not a primitive model. Introducing a counterion or hydrogen ion pressure term in the model included the effect of the counterions. The quality of the solvent was taken into account through a dimensionless polymer–polymer parameter (negative and positive for poor and good solvents, respectively). Although this model was highly simplified and not very realistic, Aalberts reported phase transitions resembling those observed by Tanaka.

Counterions, ionized groups and explicit Coulomb interactions were really considered within the primitive model by Schneider and Linse.[180,181] These authors employed the polymer network of diamond-like topology previously used by Escobedo and de Pablo. This is an ideal and defect-free structure in which the cross-linker is tetrafunctional and their interconnectivity corresponds to that of a diamond lattice. All chains are of equal length (number of monomer beads) and terminate in a cross-linker. Such perfect network permits decoupling swelling phenomena from secondary effects attributed to irregularities occurring in real polymer networks (free branches, entanglements, polydispersity,…). In any case, this topology remains unchanged throughout the course of simulations since the networks are supposed to be covalently bonded.

Through continuum-space Monte Carlo simulations, Schneider and Linse investigated the swelling behavior of polyelectrolyte gels with respect to various parameters (charge density, cross-linker density, chain flexibility, and counterion valence). According to their results, the swelling ratio increases with the charge density and the chain stiffness, whereas decreases with the cross-linker density and the counterion valence. They

also analyzed the behavior of pressure with the volume fraction and the spatial distribution of monomers, nodes and counterions.

In a subsequent paper, Schneider and Linse reported discontinuous volume phase transitions induced by short-range attractions and reductions in the dielectric constant of the solvent using the same model but including an attractive square-well potential.[181] Yin and de Pablo have also observed a discontinuous volume transition for polyelectrolyte networks at high electrostatic coupling using a similar model.[182] However, their work was mainly focused on structural aspects. Discontinuous volume transitions were also reported for uncharged hydrophobic networks.[176,177]

Mann *et al.* analyzed scaling relations for the equilibrium swelling of polyelectrolyte gels of various chain lengths and charge densities with monovalent counterions using molecular dynamics simulations within the diamond-like topology.[183] In developing these scaling relations, they concluded that only free (not condensed) counterions contributed to the osmotic pressure. In fact, they proposed a scaling relation for the end-to-end distance of the network chains that considers the counterion condensation (through an effective charge fraction) and the finite length of the chains. In their study, special emphasis was put on evaluating the electrostatic contributions to the swelling behavior, since they are neglected by the classical theories.

Yin *et al.* have investigated the effect of the valence of the counterions on the swelling behavior.[182] They simulated defect-free polyelectrolyte gels with mono-, di- and trivalent counterions (also within the primitive model and the diamond lattice topology). The swelling of polyelectrolyte gels is often explained by the balance of two effects: the elasticity of the polymer network and the osmotic pressure due to the translational entropy of the counterions. However, the results reported by Yin *et al.* suggest that this is a naïve picture and electrostatic interactions play a key role in discontinuous volume phase transitions undergone by these systems. Such transitions shift towards lower Bjerrum lengths (higher dielectric constants) with increasing the counterion valence.

The collapse of the gel has also been reported when counterions are replaced by macroions.[184] The most remarkable effect is the collapse of the gel when adding macroions up to the point of charge equivalence. After this point, the gel swells again. The initial deswelling was justified in terms of the replacement of a great number of counterions by macroions, which reduces the osmotic pressure originating from the counterions. The role of different network properties on the deswelling was also discussed.

Recently, Yin *et al.* have studied the swelling and collapse of polyelectrolyte gels in equilibrium with 1 : 1 and 2 : 1 electrolyte solutions (through grand canonical Monte Carlo).[185] Previous studies had been restricted to salt-free simulations. The swelling degree decreases with the electrolyte concentration in the reservoir (behavior observed also in experiments) and is smaller in the presence of divalent counterions. The ratio between the electrolyte concentration in the gel and the electrolyte concentration in the reservoir is also computed. In the limit of low reservoir concentrations, this quantity is surprisingly small (<10%) for monovalent electrolyte and chains of 100 (or less) monomeric units. These authors also reported the formation of a heterogeneous nanostructure (regions rich in ions coexist with regions dense in monomers).

The simulations previously commented were based on perfect networks and did not consider the solvent explicitly. Edgecombe and Linse have investigated how the polydispersity of the chain length and the topological defects in the network affect the volume and other structural properties.[186] These authors used Monte Carlo simulations and basically the same model of previous works. In general they found that polydisperse gels swell less than the perfect ones. Uncharged polymer gels are not so sensitive to the chain length polydispersity. On the other hand, the presence of chains with one end detached from the cross-linker led to an increase of the gel volume. The effect of disengaged chains was stronger for flexible polyelectrolyte gels and weaker for uncharged networks and stiff polyelectrolyte gels.

The first simulations of polyelectrolyte gels with explicit solvent particles were reported by Lu and Hentschke.[187] These authors employed a two-box-particle transfer molecular dynamics method to simulate an extremely highly cross-linked network of monomeric chains in equilibrium with a dipolar Stockmayer solvent. In their simulations, a partial charge Q was assigned to each bead of the network, whereas each neutralizing counterion had the opposite partial charge ($-Q$). Lu and Hentschke observed that the swelling ratio exhibits a broad maximum as a function of Q, which becomes less pronounced with increasing the dipole moment of the solvent particles. This non-monotonic behavior of the swelling ratio was attributed to a competition between electrostatic repulsion and the network conformational entropy.

Although computer simulations have looked into different aspects of polyelectrolyte gels, the effect of temperature has been hardly addressed. As far as we know, only Escobedo and de Pablo explicitly simulated swelling curves as a function of this property.[177] But they did it only for uncharged networks. In contrast, thermo-sensitive gels and nanogels have attracted the attention of a lot of theorists, who have developed different swelling theories for this kind of responsive materials,[188–197] mostly inspired in the Flory–Rhener formalism.[198,199] Although this issue goes beyond the scope of this review, it is worth mentioning here that these theories assumes that the free energy can be expressed as a sum of three terms reflecting the changes due to mixing, elastic and ionic effects. The expressions of these terms can vary from theory to theory. Recently, Longo *et al.* have developed a different approach based on a coarse-grained model similar to that employed in simulations,[200] which explicitly includes the contributions to the free energy of the electrostatic interaction energy arising from charged species, steric repulsions, van der Waals attractions and acid–base equilibrium. By means of entropic terms, the mixing and the conformational degrees of freedom of the chain molecule are also accounted for. This sophisticated model has been applied to the analysis of the response to pH and salt concentration. Moreover, it should be stressed that the Flory–Rhener theory can be used beyond the swelling behavior. For instance, it has been applied to mechanical properties of individual thermo-responsive microgel particles.[201]

Concerning nanogels, these particles have been explicitly simulated by Claudio *et al.*[202] In this way, these authors can calculate the actual fraction of counterions inside the network

and conclude that only half of them are situated there. This obviously confirms that the gel size (ignored in preceding simulations) can have influence on certain properties. An example of phenomenon depending on gel size is the microphase separation (swollen and shrunken regions coexist in gel), which has been theoretically studied by Jha *et al.*[203] and Wu *et al.*,[204] and was also observed in simulations by Yin *et al.*[185] Ikkai and Shibayama have proved that the microphase separation is not observed if the nanogel particle size is of the same order as the characteristic size of the microphase separation.[205]

4.2. Bicelles

Although computer simulations have been extensively applied to lipid bilayers,[22] the application to bicelles is rather scarce up to date. Two representations of reality widely used in simulations of lipid bilayers have been also employed in the case of bicelles: the atomistic models and the coarse-grained (CG) models. In the case of one and only phospholipid, atomistic simulations were carried out by several authors in their study of bilayer edges. In particular the bicelle geometry was used by Jiang *et al.* to model a bilayer edge.[206] From their simulations, results on the migration of polar headgroups, the edge morphology, or the line tension were reported. However, atomistic models present an important shortcoming: even with the actual computational resources, they are extremely time-consuming.

In GC simulations, a single bead represents some small groups of atoms. In this way, the computational time is reduced in orders of magnitude (as compared to atomistic simulations) and a meaningful exploration of the bilayer dynamics is feasible. Interactions between non-bonded beads are modeled by the Lennard-Jones (LJ) 12–6 potential, whereas chemical bonds are modeled by harmonic potentials (this is also usual in the simulation of gels).

Bicelle-like disks (as well as ribbons) composed of a mixture of short-chain and long-chain phospholipids were studied by molecular dynamics with a coarse-grained model by de Joannis *et al.*[207] The effect of system composition on the edge structure, the edge composition and the line tension was analyzed. In bilayers predominantly formed of the long-chain component, a considerable excess of the short-chain lipid at the bilayer edge and a reduction in line tension are observed. More surprisingly, in bilayers predominantly composed of short-chain lipids, there is an excess of long-chain lipids near the edge and a slight decrease in line tension compared with a bilayer of pure short-chain. Concerning the morphology, a bulge near the edge was reported (also previously seen in bicelles of pure lipid).[206]

Bicelles composed of lipid mixtures have been also simulated within atomistic models.[208,209] In this case, however, the simulations present an important shortcoming: the time required for the diffusive exchange of the different lipids exceeds the typical time for molecular dynamics trajectories. In mixtures of DMPC and DDPC, a mixed Monte Carlo/molecular dynamics method allows the equilibration of the lateral distribution of different lipid types.[208] In this approach Monte Carlo moves transform lipid molecules from one type to another extending or shortening the tail lengths. However, this method is not efficient for mixtures of DMPC and DHPC because the acceptance probability for mutation moves decreases rapidly with increasing the difference of tail length.[209] This drawback was overcome by Jiang *et al.* including a third component with intermediate tail length (DDPC) at low concentration to serve as intermediary in transitions between DMPC and DHPC.

As reported previously for DDPC/DMPC mixtures, atomistic simulations of DHPC/DMPC mixtures show the enrichment of short-chain lipid at the bicelle edge (in agreement with experiments). However, this effect is stronger for the mixture with the greatest difference in tail length (*i.e.*, DHPC/DMPC). In fact, Jiang *et al.* observe that 15% of the bicelle bulk consists of DHPC, whereas more than 40% of the edge consists of short-chain lipids. Increasing the temperature from 300 K to 323 K does not appreciably change the degree of partitioning (in contrast to experimental data). The enrichment of long-chain lipids at the edge is accompanied by an increase in edge stability. In other words, DHPC behaves as edge-active agent and reduces the excess free energy per unit of length of the edge.[209]

Due to the existence of free edges, bicelles are usually found only as unstable transient structures. In fact, these systems have been also used as starting structures in GC simulations of formation of vesicles.[210,211] On the other hand, bicelles can also be observed in studies of phase transitions of lipid mixtures. For instance, May *et al.* reported disk-shaped aggregates of lysophosphatidic acid if the concentration of Mg^{2+} is high enough.[212]

5. Conclusions and future perspectives

Nowadays works devoted to the hybrid technology are of great interest and stimuli responsive hybrid colloids containing organic and inorganic components are a matter of study due to their attractive properties. Many authors have developed new PNIPAM-based hybrid nanoparticles being a subject of several reviews.[213–215] However and as commented before, its use as a biomaterial may be limited because of the toxicity of PNIPAM and its lack of compatibility with cells and blood.

Little information is found in literature related to the VCL-based hybrid nanogels. In 2004, Pich *et al.*[216] prepared AAEM- and VCL-based hybrid temperature-sensitive nanogels. They deposited magnetite nanoparticles directly into the nanogels obtaining hybrid nanoparticles with reversible swelling-de-swelling behavior. The critical transition temperature is influenced by the amount of loaded magnetite due to the interaction of the iron oxide particles with the polymer chains of the nanogel. In 2005, Pich *et al.*[217] synthesized P(VCL-*co*-AAEM) nanogels filled with ZnS inclusions. Hybrid nanoparticles contained up to 20 wt% of ZnS, and the particle stability decreased with increased inorganic filler content. The nanogels filled with ZnS can form organized particle arrays after water evaporation. In 2007, Bhattacharya *et al.*[218] reported a simple route for the preparation of temperature-, pH- and magnetic-field-sensitive hybrid particles and observed that the presence of the magnetite nanoparticles in the nanogel decreased its degree of swelling and shifted the volume phase-transition temperature to higher values. Agrawal *et al.*[219] presented a strategy to produce ZnO loaded temperature-sensitive hybrid nanogels, which involved controlled hydrolysis of $Zn(CH_3COO)_2 \cdot 2H_2O$ salt in the presence of P(VCL-*co*-AAEM) nanogel templates in 2-propanol. The obtained hybrid nanogels had both the thermosensitive

properties of PVCL-AAEM matrix and the typical physico-chemical properties of ZnO nanoparticles.

Future work on VCL-based hybrid nanogels should be directed to produce new families of biocompatible nanogels to be used in pharmaceutical and biomedical applications.

Regarding colloidal characterization of PVCL-based nanogels, more effort should be done in the future in spite of the number of works reported in this review. Charge distribution (inside and outside of the particle) and related features (e.d.l.) still remain as open challenges. Furthermore, the pioneer aggregation experiments previously mentioned[25–27,131–135] are clearly unsatisfactory, both structure and kinetics of the PVCL-based nanogels aggregates have to be deeply elucidated. Starting from the gained experience with PNIPAM-based microgels, the study of the internal structure of PVCL-based nanogels must be encouraged. Indeed, DLS-SANS analysis should be improved in order to analyze internal motions of chains and the use of new experimental techniques should be enhanced.

As indicated above, apart from the information that one can obtain using bicelles as a membrane model in structure–function studies of membrane-associated proteins, bicelles present several advantages as possible vehicles for skin penetration. Bicellar structure contains a bilayer that allows the incorporation of substances, drugs, for instance. In other words, bicelles have a great potential as carriers for drug delivery. Only lipids compose bicelles and the presence of DHPC controlling the bicelle diameters tunes the size of the structure. Bicelles are able to penetrate through skin SC, and to interact with SC structures without promoting damage. The encapsulation of bicelles into bicosomes allows them to reach other tissues, and to have an enhancer effect on skin permeability. These nanostructures could interact with other physiological barriers, and other interactions may occur. In addition, bicosomes could be used as stabilizers, since the bicelles trapped inside can be used to support various hydrophobic drugs, such as dichlofenac.[116] The combination of the well-known characteristics of liposomes with the versatility and applicability of bicelles makes bicosomes a new and interesting strategy. All these possible fields for the application of bicelles may require a special and unique modulated system. This is the reflection of the high versatility of the bicellar systems. The potential of these systems is far beyond its initial objective of being a model membrane for studying macromolecules.

The knowledge of the properties of the bicelles from a colloidal point of view is lacking in literature, as mentioned above. The colloidal studies are in the preliminary stages, and all the properties need to be explored deeply. Future studies on lipids with a broad range of q ratios and lipid concentrations may reveal other morphologies with useful applications and ongoing efforts in theoretical models and scattering techniques should be done.

Concerning simulations, a significant progress in the understanding of the general behavior of polyelectrolyte gels has been achieved in the last decade. However, a lot of interesting work remains to be done as our attention turns to specific materials. In fact, thermo-responsive nanogels have not been explicitly simulated yet (although different theoretical approaches have been devised for them). The CG models used in simulations of bicelles (and uncharged networks) can be very useful for polyelectrolyte gels of specific materials. In any case, with the growing number of particles that can be simulated, it is expected to see an increasing collaboration between computational groups and synthetic chemists or engineers in the development of new soft nanoparticles.

Acknowledgements

First, we must not forget or fail to acknowledge that the start of this series of coordinated projects was the idea of Professor Roque Hidalgo-Álvarez. The authors also thank the Spanish Ministerio de Ciencia e Innovación (MICINN)/Programa Nacional de Materiales (MAT2009-13,155-C04-01, -02, -03, and -04). A. Imaz thanks "Ayudas de especialización para investigadores de la UPV/EHU (2007)" for financial support, and J. Ramos acknowledges financial support by the "MICINN: Subprograma Juan de la Cierva" (JCI-2008-2217). J. Forcada and A. Imaz also thank the project FONCICYT-96095. J. Callejas-Fernández and M. Quesada-Pérez acknowledge the project P07-FQM-02496 from Junta de Andalucía.

References

1 B. R. Saunders and B. Vincent, *Adv. Colloid Interface Sci.*, 1999, **80**, 1–25.
2 R. Pelton, *Adv. Colloid Interface Sci.*, 2000, **85**, 1–33.
3 H. G. Schild, *Prog. Polym. Sci.*, 1992, **17**, 163–249.
4 J. Zhou, G. Wang, L. Zou, L. Tang, M. Marquez and Z. Hu, *Biomacromolecules*, 2008, **9**, 142–148.
5 M. Das, S. Mardyani, W. C. W. Chan and E. Kumacheva, *Adv. Mater.*, 2006, **18**, 80–83.
6 T. Hoare and R. Pelton, *Langmuir*, 2008, **24**, 1005–1012.
7 W. Qin, Y. Zhao, Y. Yang, H. Xu and X. Yang, *Colloid Polym. Sci.*, 2007, **285**, 515–521.
8 C. M. Nolan, C. D. Reyes, J. D. Debord, A. J. Garcia and L. A. Lyon, *Biomacromolecules*, 2005, **6**, 2032–2039.
9 V. Castro Lopez, J. Hadgraft and M. J. Snowden, *Int. J. Pharm.*, 2005, **292**, 137–147.
10 M. Das, N. Sanson, D. Fava and E. Kumacheva, *Langmuir*, 2007, **23**, 196–201.
11 G. E. Morris, B. Vincent and M. J. Snowden, *J. Colloid Interface Sci.*, 1997, **190**, 198–205.
12 M. Bradley, J. Ramos and B. Vincent, *Langmuir*, 2005, **21**, 1209–1215.
13 H. Vihola, A. Laukkanen, L. Valtola, H. Tenhu and J. Hirvonen, *Biomaterials*, 2005, **26**, 3055–3064.
14 L. Jun, W. Bochu and W. Yazhou, *Int. J. Pharmacol.*, 2006, **2**, 513–519.
15 A. Laukkanen, L. Valtola, F. M. Winnik and H. Tenhu, *Macromolecules*, 2004, **37**, 2268–2274.
16 A. Imaz and J. Forcada, *J. Polym. Sci., Part A: Polym. Chem.*, 2010, **48**, 1173–1181.
17 M. N. Triba, D. E. Warschawski and P. F. Devaux, *Biophys. J.*, 2005, **88**, 1887–1901.
18 L. van Dam, G. Karlsson and K. Edwards, *Langmuir*, 2006, **22**, 3280–3285.
19 A. Pich, A. Tessier, V. Boyko, Y. Lu and H.-J. P. Adler, *Macromolecules*, 2006, **39**, 7701–7707.
20 J. Katsaras, T. A. Harroun, J. Pencer and M.-P. Nieh, *Naturwissenschaften*, 2005, **92**, 355–366.
21 A. V. Dobrynin, *Curr. Opin. Colloid Interface Sci.*, 2008, **13**, 276.
22 S. J. Marrink, A. H. de Vries and D. P. Tieleman, *Biochim. Biophys. Acta*, 2009, **1788**, 149.
23 F. A. Escobedo and J. J. de Pablo, *Phys. Rep.*, 1999, **318**, 85.
24 Y. Gao, S. C. F. Au-Yeng and C. Wu, *Macromolecules*, 1999, **32**, 3674–3677.
25 S. Peng and C. Wu, *Macromol. Symp.*, 2000, **159**, 179–186.
26 S. Peng and C. Wu, *Macromolecules*, 2001, **34**, 568–571.
27 S. Peng and C. Wu, *Polymer*, 2001, **42**, 7343–7347.
28 H. Vihola, A.-K. Marttila, J. S. Pakkanen, M. Andersson, A. Laukkanen, A. M. Kaukonen, H. Tenhu and J. Hirvonen, *Int. J. Pharm.*, 2007, **343**, 238–246.

29 V. Boyko, S. Richter, A. Pich and K.-F. Arndt, *Colloid Polym. Sci.*, 2003, **282**, 127–132.
30 V. Boyko, S. Richter, I. Grillo and E. Geissler, *Macromolecules*, 2005, **38**, 5266–5270.
31 A. Laukkanen, S. Hietala, S. L. Maunu and H. Tenhu, *Macromolecules*, 2000, **33**, 8703–8708.
32 A. Imaz and J. Forcada, *J. Polym. Sci., Part A: Polym. Chem.*, 2008, **46**, 2510–2524.
33 A. Imaz and J. Forcada, *J. Polym. Sci., Part A: Polym. Chem.*, 2008, **46**, 2766–2775.
34 A. Imaz and J. Forcada, *Eur. Polym. J.*, 2009, **11**, 3164–3175.
35 V. Boyko, A. Pich, Y. Lu, S. Richter, K.-F. Arndt and H.-J. P. Adler, *Polymer*, 2003, **44**, 7821–7827.
36 A. Pich, Y. Lu, V. Boyko, K.-F. Arndt and H.-J. P. Adler, *Polymer*, 2003, **44**, 7651–7659.
37 S. Schachschal, A. Balaceanu, C. Melian, D. E. Demco, T. Eckert, W. Richtering and A. Pich, *Macromolecules*, 2010, **43**, 4331–4339.
38 Y. E. Kirsh, N. A. Yanul and K. K. Kalninsh, *Eur. Polym. J.*, 1999, **35**, 305–316.
39 A. Imaz, J. Miranda, J. Ramos and J. Forcada, *Eur. Polym. J.*, 2008, **44**, 4002–4011.
40 L. M. Mikheeva, N. V. Grinberg, A. Y. Mashkevich, V. Y. Grinberg, L. T. M. Thanh, E. E. Makhaeva and A. R. Khokhlov, *Macromolecules*, 1997, **30**, 2693–2699.
41 R. Blankenburg and A. Sanner, *Deuts. Pat.*, 4342281-A1, 1995.
42 R. Blankenburg and A. Sanner, *Eur. Pat.*, 709411-A2, 1996.
43 A. Boettcher, R. Pinkos, R. E. Lorenz, H. Becker and A. Bottcher, *Deuts. Pat.*, 10223968-A1, 2002.
44 J. Kroker, R. Schneider, E. Schupp and M. Kerber, *US Pat.*, 005739195, 2008.
45 M. Schrod, *Deuts. Pat.*, 10254432-A1, 2004.
46 J. Chuang, J. S. Shih and M. A. Drzewinski, *US Pat.*, 2003008993–A1, 2003.
47 T. Ohsumi, *WO Pat.*, 9509899–A1, 1995.
48 L. K. Kostanski, R. X. Huang, R. Ghosh and C. D. M. Filipe, *J. Biomater. Sci., Polym. Ed.*, 2008, **19**, 275–290.
49 M. Prabaharan, J. J. Grailer, D. A. Steeber and S. Q. Gong, *Macromol. Biosci.*, 2009, **9**, 744–753.
50 D. Crespy, A. Golosova, E. Makhaeva, A. R. Khokhlov, G. Fortunato and R. Rossi, *Polym. Int.*, 2009, **58**, 1326–1334.
51 A. Moshaverinia, N. Roohpour, J. A. Darr and I. U. Rehman, *Acta Biomater.*, 2009, **6**, 2101–2108.
52 K. J. Crowell and P. M. MacDonald, *Biochim. Biophys.Acta*, 1999, **1416**, 21–30.
53 J. Struppe, J. A. Whiles and R. R. Vold, *Biophys. J.*, 2000, **78**, 281–289.
54 I. Marcotte, E. J. Dufourc, M. Ouellet and M. Auger, *Biophys. J.*, 2003, **85**, 328–339.
55 E. K. Tiburu, D. M. Moton and G. A. Lorigan, *Biochim. Biophys. Acta*, 2001, **1512**, 206–214.
56 M. A. Parker, V. King and K. P. Howard, *Biochim. Biophys. Acta*, 2001, **1514**, 206–212.
57 H. S. Cho, J. L. Dominick and M. M. Spence, *J. Phys. Chem.*, 2010, **114**, 9238–9245.
58 C. R. Sanders and J. H. Prestegard, *Biophys. J.*, 1990, **58**, 447–460.
59 R. R. Vold and R. S. Prosser, *J. Magn. Reson., Ser. B*, 1997, **113**, 267–271.
60 L. Barbosa-Barros, A. de la Maza, J. Estelrich, A. M. Linares, M. Feliz, P. Walther, R. Pons and O. López, *Langmuir*, 2008, **24**, 5700–5706.
61 J. Struppe and R. R. Vold, *J. Magn. Reson.*, 1998, **135**, 541–546.
62 I. Marcotte and M. Auger, *Concepts Magn. Reson.*, 2005, **24**, 17–37.
63 J. A. Whiles, R. Brasseur, K. J. Glover, G. Melacini, E. A. Komives and R. R. Vold, *Biophys. J.*, 2001, **80**, 280–293.
64 K. J. Glover, J. A. Whiles, M. J. Wood, G. Melacini and E. A. Komives, *Biochemistry*, 2001, **40**, 13137–13142.
65 R. R. Vold, R. S. Proser and A. J. Deese, *J. Biomol. NMR*, 1997, **9**, 329–335.
66 K. J. Glover, J. A. Whiles, R. R. Vold and G. Melacini, *J. Biomol. NMR*, 2002, **22**, 57–64.
67 C. R. Sanders, II and K. Oxenoid, *Biochim. Biophys. Acta*, 2000, **1508**, 129–145.
68 P. A. Luchette, T. N. Vetman, R. S. Proser, R. Hancock, M. P. Nieh, C. J. Glinka, S. Krueger and J. Katsaras, *Biochim. Biophys. Acta*, 2001, **1513**, 83–94.
69 K. J. Glover, J. A. Whiles, G. H. Wu, N. J. Yu, R. A. Deems, J. O. Struppe, R. E. Stark, E. A. Komives and R. R. Vold, *Biophys. J.*, 2001, **81**, 2163–2171.
70 M. P. Nieh, V. A. Raghunathan, C. J. Glinka, T. A. Harroun, G. Pabst and J. Katsaras, *Langmuir*, 2004, **20**, 7893–7897.
71 L. Barbosa-Barros, A. de la Maza, P. Walther, A. M. Linares, M. Feliz, J. Estelrich and O. López, *J. Microsc.*, 2009, **233**(Pt 1), 35–41.
72 C. R. Sanders, B. J. Hare, K. P. Howard and J. H. Prestegard, *Prog. Nucl. Magn. Reson. Spectrosc.*, 1994, **26**, 421–444.
73 M. Ottiger and A. Bax, *J. Biomol. NMR*, 1998, **12**, 361–372.
74 E. Boroske and W. Helfrich, *Biophys. J.*, 1978, **24**, 863–868.
75 C. R. Sanders and G. C. Landis, *Biochemistry*, 1995, **43**, 4030–4040.
76 K. P. Howard and S. J. Opella, *J. Magn. Reson.*, 1996, **112**, 91–94.
77 J. A. Lesonczi and J. H. Prestegard, *Biochemistry*, 1998, **37**, 706–716.
78 J. Struppe, E. H. Komives, S. S. Taylor and R. R. Vold, *Biochemistry*, 1998, **37**, 15523–15527.
79 R. S. Prosser, S. A. Hunt, J. A. DiNatale and R. R. Vold, *J. Am. Chem. Soc.*, 1996, **118**, 269–270.
80 R. S. Prosser and I. V. Shiyanovskaya, *Concepts Magn. Reson.*, 2001, **13**, 19–31.
81 R. S. Prosser, V. B. Volkov and I. V. Shiyanovskaya, *Biochem. Cell. Biol.*, 1998, **76**, 443–451.
82 R. S. Prosser, V. B. Volkov and I. V. Shiyanovskaya, *Biophys. J.*, 1998, **75**, 2163–2169.
83 J. A. Whiles, R. Deems, R. R. Vold and E. A. Dennis, *Bioinorg. Chem.*, 2002, **30**, 431–442.
84 M. Seigneuret and D. Levy, *J. Biomol. NMR*, 1995, **5**, 345–352.
85 D.-K. Chang, S.-F. Cheng and W. J. Chien, *J. Virol.*, 1997, **71**, 6593–6602.
86 M. R. Tessmer, J. P. Meyer, V. J. Hruby and D. A. Kallick, *J. Med. Chem.*, 1997, **40**, 2148–2155.
87 B. Bechinger, M. Zasloff and S. J. Opella, *Biophys. J.*, 1998, **74**, 981–987.
88 E. Barany-Wallje, A. Anderson, A. Graeslund and L. Mäler, *FEBS Lett.*, 2004, **567**, 265–269.
89 M. Lindberg, H. Biverståhl, A. Graäslund and L. Mäler, *Eur. J. Biochem.*, 2003, **270**, 3055–3063.
90 C. R. Sandres and J. P. Schwonek, *Biochemistry*, 1992, **31**, 8898–8905.
91 F. Picard, M.-J. Paquet, J. Levesque, A. Belanger and M. Auger, *Biophys. J.*, 1999, **77**, 888–902.
92 M.-P. Nieh, C. J. Glinka, S. Krueger, R. S. Prosser and J. Katsaras, *Biophys. J.*, 2002, **82**, 2487–2498.
93 E. K. Tiburu, P. C. Dave and G. A. Lorigan, *Magn. Reson. Chem.*, 2004, **42**, 132–138.
94 I. Marcotte, K. L. Wegener, Y.-H. Lam, B. C. S. Chia, M. R. R. de Planque, J. H. Bowie, M. Auger and F. Separovic, *Chem. Phys. Lipids*, 2003, **122**, 107–120.
95 J. Guo, S. Pavlopoulos, X. Tian, D. Lu, S. P. Nikas, D.-P. Yang and A. Makriyannis, *J. Med. Chem.*, 2003, **46**, 4838–4846.
96 F. Aussenac, M. Laguere, J.-M. Schmitter and E. J. Dufourc, *Langmuir*, 2003, **19**, 10468–10479.
97 R. S. Prosser, H. Bryant, R. G. Bryant and R. R. Vold, *J. Magn. Reson.*, 1999, **14**, 256–260.
98 H. Sasaki, S. Fukuzawa, J. Kikuchi, S. Yokoyama, H. Hirota and K. Tachibana, *Langmuir*, 2003, **19**, 9841–9844.
99 C. Sizun, F. Aussenac, A. Grelard and E. J. Dufourc, *Magn. Reson. Chem.*, 2004, **42**, 180–186.
100 J. A. Whiles, K. J. Glover, R. R. Vold and E. A. Komives, *J. Magn. Reson.*, 2002, **158**, 149–156.
101 A. Andersson and L. Mäler, *J. Biomol. NMR*, 2002, **24**, 103–112.
102 A. Andersson and L. Mäler, *FEBS Lett.*, 2003, **545**, 139–143.
103 A. Andersson and L. Mäler, *Biochim. Biophys. Acta*, 2004, **1661**, 18–25.
104 L. Barbosa-Barros, C. Barba, M. Cócera, L. Coderch, C. López-Iglesias, A. de la Maza and O. López, *Int. J. Pharm.*, 2007, **352**, 263–272.
105 C. C. Muller-Goymann, *Eur. J. Pharm. Biopharm.*, 2004, **58**, 343–356.
106 M. M. Elsayed, O. Y. Abdallah, V. F. Naggar and N. M. Khalafallah, *Int. J. Pharm.*, 2007, **332**, 1–16.
107 H. A. E. Benson, *Curr. Drug Delivery*, 2005, **2**, 23–33.
108 F. Kartono and H. I. Maibach, *Contact Dermatitis*, 2006, **54**, 303–312.

109 L. Barbosa-Barros, A. de la Maza, C. López-Iglesias and O. López, *Colloids Surf., A*, 2007, **317**, 576–584.
110 L. Barbosa-Barros, A. de la Maza, P. Walther, J. Estelrich and O. López, *J. Microsc.*, 2007, **230**, 16–26.
111 L. Coderch, O. López, A. de la Maza and J. L. Parra, *Am. J. Clin. Dermatol.*, 2002, **4**, 107–129.
112 C. L. Gay, R. H. Guy, G. M. Golden, V. H. W. Mak and M. L. Francoeur, *J. Invest. Dermatol.*, 1994, **103**, 233–239.
113 M. M. Koan and G. J. Blanchard, *J. Phys. Chem. B*, 2006, **110**, 16584–16590.
114 G. M. El Maghraby, M. Campbell and B. C. Finn, *Int. J. Pharm.*, 2005, **305**, 90–104.
115 G. Rodríguez, L. Barbosa-Barros, L. Rubio, M. Cócera, A. Díez, J. Estelrich, R. Pons, J. Caelles, A. de la Maza and O. López, *Langmuir*, 2009, **25**, 10595–10603.
116 L. Rubio, C. Alonso, G. Rodríguez, L. Barbosa-Barros, L. Coderch, A. de la Maza, J. L. Parra and O. López, *Int. J. Pharm.*, 2010, **386**, 108–113.
117 G. Rodríguez, G. Soria, E. Coll, L. Rubio, L. Barbosa-Barros, C. López-Iglesias, A. M. Planas, J. Estelrich, A. de la Maza and O. López, *Biophys. J.*, 2010, **99**, 480–488.
118 B. J. Berne and R. Pecora, in *Dynamic Light Scattering with Applications to Chemistry, Biology and Physics*, R.E. Krieger Publishing Company, Malabar, Reprint edn, 1990, ch. 8, pp. 164–206.
119 P. N. Pusey and R. J. A. Tough, in *Dynamic Light Scattering. Applications of Photon Correlation Spectroscopy*, ed. R. Pecora, Plenum, New York, 1st edn, 1985, ch. 4, pp. 85–142.
120 B. Chu, in *Laser Light Scattering: Basic Principles and Practice*, Dover, London, 2nd edn, 1991, ch. 7, pp. 243–280.
121 A. C. W. Lau and C. Wu, *Macromolecules*, 1999, **32**, 581–584.
122 P. C. Hiemenz and R. Rajagopalan, in Principles of Colloid and Surface Chemistry, Marcel Dekker, New York, 3rd edn, 1997, ch. 5, pp. 193–243.
123 M. Kerker, in *The Scattering of Light and other Electromagnetic Radiation*, Academic Press, Orlando, 1st edn, 1969, ch. 8, pp. 414–486.
124 T. Hoare and R. Pelton, *J. Phys. Chem. B*, 2006, **110**, 20327–20336.
125 T. Hoare and R. Pelton, *Langmuir*, 2006, **22**, 7342–7350.
126 T. Hoare and R. Pelton, *Langmuir*, 2004, **20**, 2123–2133.
127 F. Ikkai, T. Suzuki, T. Karino and M. Shibayama, *Macromolecules*, 2007, **40**, 1140–1146.
128 Y. Li, R. de Vries, T. Slaghek, J. Timmermans, M. A. Cohen Stuart and W. Norde, *Biomacromolecules*, 2009, **10**, 1931–1938.
129 A. Fernández-Nieves and M. Márquez, *J. Chem. Phys.*, 2005, **122**, 084702.
130 B. Sierra-Martín, M. S. Romero-Cano, A. Fernández-Nieves and A. Fernández-Barbero, *Langmuir*, 2006, **22**, 3586–3590.
131 S. Peng and C. Wu, *Polymer*, 2001, **42**, 6871–6876.
132 S. Peng and C. Wu, *J. Phys. Chem. B*, 2001, **105**, 2331–2335.
133 S. Peng and C. Wu, *Polymer*, 2003, **44**, 1089–1093.
134 H. C. Cheng, C. Wu and M. A. Winnik, *Macromolecules*, 2004, **37**, 5127–5129.
135 A. Laukkanen, S. K. Wiedmer, S. Varjo, M. L. Riekkola and H. Tenhu, *Colloid Polym. Sci.*, 2002, **280**, 65–70.
136 D. Kunz and W. Burchard, *Colloid Polym. Sci.*, 1986, **264**, 498–506.
137 X. Wu, R. H. Pelton, A. E. Hamielec, D. R. Woods and W. McPhee, *Colloid Polym. Sci.*, 1994, **272**, 467–477.
138 K. Kratz, T. Hellweg and W. Eimer, *Polymer*, 2001, **42**, 6631–6639.
139 K. Kratz, A. Lapp, W. Eimer and T. Hellweg, *Colloids Surf., A*, 2002, **197**, 55–67.
140 I. Varga, T. Gilányi, R. Mészáros, G. Filipcsei and M. Zrínyi, *J. Phys. Chem. B*, 2001, **105**, 9071–9076.
141 A. Fernández-Barbero, A. Fernández-Nieves, I. Grillo and E. López-Cabarcos, *Phys. Rev. E: Stat., Nonlinear, Soft Matter Phys.*, 2002, **66**, 051803.
142 B. Saunders, *Langmuir*, 2004, **20**, 3925–3932.
143 M. Stieger, W. Richtering, J. S. Pedersen and P. Lindner, *J. Chem. Phys.*, 2004, **120**, 6197–6206.
144 J. S. Pedersen and C. Svaneborg, *Curr. Opin. Colloid Interface Sci.*, 2002, **7**, 158–166.
145 M. Olvera de la Cruz, *Soft Matter*, 2008, **4**, 1735–1739.
146 D. Gottwald, C. N. Likos, G. Kahl and H. Löwen, *Phys. Rev. Lett.*, 2004, **92**, 068301.
147 S. Sorlie and R. Pecora, *Macromolecules*, 1988, **21**, 1437–1449.
148 C. Han and A. Z. Akcasu, *Macromolecules*, 1981, **14**, 1080–1084.
149 C. Wu and S. Zhou, *Macromolecules*, 1996, **29**, 1574–1578.
150 V. Boyko, S. Richter, W. Burchard and K. F. Arndt, *Langmuir*, 2007, **23**, 776–784.
151 M.-P. Nieh, T. A. Harroun, V. A. Raghunathan, C. J. Glinka and J. Katsaras, *Biophys. J.*, 2004, **86**, 2615–2629.
152 B. Yue, C.-Y. Huang, M.-P. Nieh, C. J. Glinka and J. Katsaras, *J. Phys. Chem.*, 2005, **109**, 609–816.
153 S. K. Wiedmer and R. Shimmo, *Electrophoresis*, 2009, **30**, S240–S257.
154 R. L. Owen, J. K. Strasters and E. D. Breyer, *Electrophoresis*, 2005, **26**, 735–751.
155 K. Kawakami, Y. Nishihara and K. Hirano, *J. Colloid Interface Sci.*, 1998, **206**, 177–180.
156 L. A. Holland and A. M. Leigh, *Electrophoresis*, 2003, **24**, 2935–2939.
157 E. Boija, A. Lundquist, M. Nilsson, K. Edwards, R. Isaksson and G. Johansson, *Electrophoresis*, 2008, **29**, 3377–3383.
158 T. Sikanen, S. K. Wiedmer, L. Heikkilä, S. Franssila, R. Kostiainen and T. Kotiaho, *Electrophoresis*, 2010, **31**, 2566–2574.
159 N. E. Gabriel and M. F. Roberts, *Biochemistry*, 1986, **25**, 2812–2821.
160 N. E. Gabriel and M. F. Roberts, *Biochemistry*, 1987, **26**, 2432–2440.
161 J. R. Bian and M. F. Roberts, *Biochemistry*, 1990, **29**, 7928–7935.
162 P. Ram and J. H. Prestegard, *Biochim. Biophys. Acta*, 1988, **940**, 289–294.
163 C. R. Sanders and R. Scott Prosser, *Structure*, 1998, **6**, 1227–1234.
164 C. R. Sanders, in *Modern Magnetic Resonance*, ed. G. A. Webb, Springer, Dordrecht, 1st edn, 2008, vol. 1., ch. 9, pp. 233–239.
165 B. J. Hare, J. H. Prestegard and D. M. Engelman, *Biophys. J.*, 1995, **69**, 1891–1896.
166 J. Chung and J. Prestegard, *J. Phys. Chem.*, 1993, **97**, 9837–9843.
167 M.-P. Nieh, C. J. Glinka, S. Krueger, R. S. Prosser and J. Katsaras, *Langmuir*, 2001, **17**, 2629–2638.
168 G. Raffard, S. Steinbruckner, A. Arnold, J. H. Davis and E. J. Dufourc, *Langmuir*, 2000, **16**, 7655–7662.
169 J. Boltze, T. Fujisawa, T. Nagao, K. Norisada, H. Saitô and A. Naito, *Chem. Phys. Lett.*, 2000, **329**, 215–220.
170 S. Gaemers and A. Bax, *J. Am. Chem. Soc.*, 2001, **123**, 12343–12352.
171 R. Soong and P. M. McDonald, *Biophys. J.*, 2005, **88**, 255–268.
172 R. Soong and P. M. McDonald, *Langmuir*, 2009, **25**, 380–390.
173 E. O. Stejskal and J. E. Tanner, *J. Chem. Phys.*, 1965, **42**, 288–295.
174 F. A. Escobedo and J. J. de Pablo, *J. Chem. Phys.*, 1996, **104**, 4788.
175 F. A. Escobedo and J. J. de Pablo, *Mol. Phys.*, 1997, **90**, 437.
176 F. A. Escobedo and J. J. de Pablo, *J. Chem. Phys.*, 1997, **106**, 793.
177 F. A. Escobedo and J. J. de Pablo, *J. Chem. Phys.*, 1999, **110**, 1290.
178 T. Tanaka, D. Fillmore, S.-T. Sun, I. Nishio, G. Swislow and A. Shah, *Phys. Rev. Lett.*, 1980, **45**, 1636.
179 D. P. Aalberts, *J. Chem. Phys.*, 1996, **104**, 4309.
180 S. Schneider and P. Linse, *J. Phys. Chem. B*, 2003, **107**, 8030.
181 S. Schneider and P. Linse, *Macromolecules*, 2004, **37**, 3850.
182 D. W. Yin, Q. Yan and J. J. de Pablo, *J. Chem. Phys.*, 2005, **123**, 174909.
183 B. A. Mann, C. Holm and K. Kremer, *J. Chem. Phys.*, 2005, **122**, 154903.
184 S. Edgecombe and P. Linse, *Langmuir*, 2006, **22**, 3836.
185 D. W. Yin, M. Olvera de la Cruz and J. J. de Pablo, *J. Chem. Phys.*, 2009, **131**, 194907.
186 S. Edgecombe and P. Linse, *Macromolecules*, 2007, **40**, 3868–3875.
187 Z. Y. Lu and R. Hentschke, *Phys. Rev. E: Stat., Nonlinear, Soft Matter Phys.*, 2003, **67**, 061807.
188 S. Hirotsu, Y. Hirokawa and T. Tanaka, *J. Chem. Phys.*, 1987, **87**, 1392–1395.
189 K. Otake, H. Inomata, M. Konno and S. Saito, *J. Chem. Phys.*, 1989, **91**, 1345–1350.
190 M. Marchetti, S. Prager and E. L. Cussler, *Macromolecules*, 1990, **23**, 1760–1765.
191 M. Shibayama and T. Tanaka, Phase Transitions and Related Phenomena of Polymer Gel, in *Responsive Gels: Volume Transitions I*, ed. K. Dusek, Springer-Verlag, Berlin, 1993.
192 A. K. Lele, I. Devotta and R. A. Mashelkar, *J. Phys. Chem.*, 1997, **106**, 4768–4772.
193 T. Hino and J. M. Prausnitz, *Polymer*, 1998, **39**, 3279–3283.
194 Y. P. Hohng and Y. C. Bae, *J. Polym. Sci., Part B: Polym. Phys.*, 2002, **40**, 2333–2338.
195 H. Li, X. Wang, G. Yan, K. Y. Lam, S. Cheng, T. Zou and R. Zhuo, *Chem. Phys.*, 2005, **309**, 201–208.

196 Y. Huang, X. Jin, H. Liu and Y. Hu, *Fluid Phase Equilib.*, 2008, **263**, 96–101.
197 S. C. Jung, S. Y. Oh and Y. C. Bae, *Polymer*, 2009, **50**, 3370–3377.
198 P. J. Flory and J. Rehner, *J. Chem. Phys.*, 1943, **11**, 512–520.
199 P. J. Flory and J. Rehner, *J. Chem. Phys.*, 1943, **11**, 521–526.
200 G. Longo, M. Olvera de la Cruz and I. Szleifer, *Macromolecules*, 2011, **44**, 147–158.
201 S. M. Hasmi and E. R. Dufresne, *Soft Matter*, 2009, **5**, 3682–3688.
202 G. C. Claudio, K. Kremer and C. Holm, *J. Chem. Phys.*, 2009, **131**, 094903.
203 P. K. Jha, F. J. Solis, J. J. de Pablo and M. Olvera de la Cruz, *Macromolecules*, 2009, **42**, 6284–6289.
204 K. A. Wu, P. K. Jha and M. Olvera de la Cruz, *Macromolecules*, 2010, **43**, 9160–9167.
205 F. Ikkai and M. Shibayama, *Polymer*, 2007, **48**, 2387–2394.
206 F. Y. Jiang, Y. Bouret and J. T. Kindt, *Biophys. J.*, 2004, **87**, 182.
207 J. de Joannis, F. Y. Jiang and J. T. Kindt, *Langmuir*, 2006, **22**, 998.
208 H. Wang, J. de Joannis, Y. Jiang, J. C. Gaulding, B. Albrecht, F. Yin, K. Khanna and J. T. Kindt, *Biophys. J.*, 2008, **95**, 2647.
209 Y. Jiang, H. Wang and J. T. Kindt, *Biophys. J.*, 2010, **98**, 2895.
210 S. J. Marrink and A. E. Mark, *J. Am. Chem. Soc.*, 2003, **125**, 15233.
211 A. J. Markvoort, K. Pieterse, M. N. Steijaert, P. Spijker and P. A. J. Hilbers, *J. Phys. Chem. B*, 2005, **109**, 22649.
212 E. R. May, D. I. Kopelevich and A. Narang, *Biophys. J.*, 2008, **94**, 878.
213 A. Pich and H.-J. P. Adler, *Polym. Int.*, 2007, **56**, 291–307.
214 M. Karg and T. Hellweg, *Curr. Opin. Colloid Interface Sci.*, 2009, **14**, 438–450.
215 M. Karg and T. Hellweg, *J. Mater. Chem.*, 2009, **19**, 8714–8727.
216 A. Pich, S. Bhattacharya, Y. Lu, V. Boyko and H.-J. P. Adler, *Langmuir*, 2004, **20**, 10706–10711.
217 A. Pich, J. Hain, Y. Lu, V. Boyko, Y. Prots and H.-J. P. Adler, *Macromolecules*, 2005, **38**, 6610–6619.
218 S. Bhattacharya, F. Eckert, V. Boyko and A. Pich, *Small*, 2007, **4**, 650–657.
219 M. Agrawal, A. Pich, S. Gupta, N. E. Zafeiropoulos, J. Rubio-Retama, F. Simon and M. Stamm, *J. Mater. Chem.*, 2008, **18**, 2581–2586.

